Mechanical Strength Studies of Steady-State Thermal and Pulsed Laser Tissue Welding

Sean D. Pearson
B. S. New Mexico State University, 1994

A thesis submitted to the faculty of the
Oregon Graduate Institute of Science & Technology
in partial fulfillment of the
requirements for the degree
Master of Science
in
Electrical Engineering

April 1996

The thesis "Mechanical Strength Studies of Steady-State Thermal and Pulsed Laser Tissue Welding" by Sean D. Pearson has been examined and approved by the following Examination Committee:

Scott Prahl
Assistant Professor
Thesis Research Advisor

Kenton Gregory
Director, Oregon Medical Laser Center

Rao Gudimetla
Assistant Professor

Dedication

To my wife, Rachael Tingen, for all of her love and support during the two-year-long tunnel of my graduate work. And to my parents, Ron and Diane Pearson, for all of their encouragement.

Acknowledgements

I would like to thank the Oregon Medical Laser Center and Dr. Ken Gregory for the lab equipment and support. I thank Andrew Barofsky for all the help with the different tissue materials, as well as Elaine LaJoie and Ujwal Sathyam for all the computer and LaTeX help. I would also like to thank the rest of the staff for all their support, and keeping me sane!!! Lastly, I would like to especially thank Dr. Scott Prahl for his encouragement and guidance through the highs and lows of graduate life.

Contents

List of Tables

List of Figures

Abstract

Mechanical Strength Studies of Steady-State Thermal and Pulsed Laser Tissue Welding

Sean D. Pearson, M.S.
Oregon Graduate Institute of Science & Technology, 1996

Supervising Professor: Scott Prahl

Laser tissue welding is the process of binding two tissues together using laser irradiation with a mechanism that is still poorly understood. This study examined the mechanism of laser welding by determining the effects of heat and pulsed diode laser light on tissue. This includes yield strength tests, steady-state thermal contraction/expansion tests, and waterbath and laser welding experiments.

Yield strength measurements indicated that porcine aorta and intestine have great variations in yield due to structural and thickness variability. Waterbath heating experiments demonstrated that initial heating had little effect on average yield strength, while laser yield tests indicated a 20% decrease in average yield strength. Also, yield strength was inversely proportional to number of pulses: i.e. the more pulses fired, the lower the yield strength.

Porcine aorta, intestine and elastin biomaterial react differently to immersion in hot water. Porcine intestine contracted at an exponential rate of 0.6 ± 0.1 (s^{-1}) above a threshold temperature of 77 ± 1°C. Aorta contracted at two different rates, the first at a rate of 0.07 ± 0.03 (s^{-1}) above a threshold temperature of 65 ± 5°C and the second at a

slightly increasing linear rate of 0.0005 ± 0.0001 (1/s°C). The elastin biomaterial actually elongated with increasing temperature at a linear rate of 0.036 ± 0.006 (1/s°C). Laser contraction was performed on porcine aorta and intestine stained with 6.5 mM ICG. Results show contraction occurred only after 10 pulses at irradiances above 75 mJ/mm^2, and maximized at 2–3 mm.

Waterbath welds were performed on all five combinations of intestine, aorta, and heterograft at temperatures from 50–80°C and times in the range of 3–15 minutes. All welds peaked at temperatures of 70–75°C, and all intestine type welds peaked at 10 minutes. The others have time peaks beyond the times used in these studies.

Laser welds were attempted on all waterbath weld types with success in all types except aorta-aorta welds. Laser weld strengths peaked at staining concentrations of 1.6 mM, irradiances of 42 mJ/mm^2, and high pulse numbers (above 10 pulses). Peak laser weld strengths were 30–100% of waterbath weld strengths.

Mechanical strength tests provided a basis for thermal effects on tissue strength. Thermal contraction/expansion studies produced different mechanisms for thermal changes in each tissue type. The waterbath and laser welding studies provided a basis for the strongest welds possible between each tissue type, as well as two viable methods to produce tissue welds. The welding tests also lead to separate mechanisms for welding due to large differences in peak welding times and temperatures.

Nomenclature

A The frequency factor (s^{-1})

c heat capacity (J/gm)

d depth of the stained layer (μm)

E irradiance (mJ/mm^2)

$n(0)$ The number of native molecule originally present (unitless)

$n(t)$ The number of native molecule at time t (unitless)

T Temperature (K)

t Heating time (s)

V_s voltage for stained tissue (mV)

V_u voltage for unstained tissue (mV)

x Length (mm)

x_{end} ending length (mm)

x_{norm} normalized position (unitless)

x_{start} starting length (mm)

α The exponential contraction rate (s^{-1})

ΔE The activation energy (J/mol)

ΔH The change in enthalpy of reaction (J/mol)

ΔS The change in entropy of reaction (J/s)

ΔT change in temperature (°C)

ϵ change in length over starting length (unitless)

κ thermal diffusivity (cm^2/s)

μ_a absorption coefficient (cm^{-1})

$\Omega(t)$ Accumulated damage (unitless)

ρ density (gm/cm^3)

$\mathcal{T}_s$ Transmission of stained tissue (unitless)

$\mathcal{T}_u$ Transmission of unstained tissue (unitless)

Chapter 1

Introduction

Laser welding of tissues has been performed with varying degrees of success for over a decade, encompassing a large realm of lasers, tissues, and methods. Successful welds have been produced with argon, Nd:YAG, THC:YAG, and CO_2 lasers on tissues such as artery, intestine, colon, and ureter [1–3]. The advantages over traditional methods of wound closure include no foreign body reaction, complete sealing of the wound, and decreased healing time [4]. One major disadvantage, examined in this study, is the difficulty of reproducibly creating a strong, reliable weld, due to a poor understanding of the laser welding mechanism.

1.1 Goals

The overall goal of this research is to produce laser welds of consistent strength and durability, so that welding can become a clinically viable means of wound closure. Specifically, the mechanism of laser welding must be understood. Therefore, we must identify the components in tissue that are responsible for welding and determine how their optical, physical, thermal, and chemical characteristics are affected when exposed to laser light. To achieve this characterization, a number of smaller goals must be reached first. Each different tissue requires mechanical testing to determine its strength initially, and its variation in strength when exposed to heat or laser light. Detailed thermal exposure experiments need to be performed to characterize the effect of temperature on tissue components thought to be responsible for welding. These studies will help pinpoint

changes that occur in each different tissue due to temperature, therefore narrowing the optimum welding temperature range.

Once each tissue has been characterized, several welds must be attempted to determine the best parameters. This is done with a series of waterbath (steady-state) and laser welding attempts. The waterbath welds will provide optimal temperatures for welding, as well as a basis for the strongest welds possible for each tissue type. The laser welds will provide the optimal parameters that produce the strongest laser weld for each tissue type. An accurate, reliable, and easy strength testing method must also be found. Lastly, welds created with the laser parameters must be tested for reliability, so that welding can eventually become a viable alternative to sutures.

1.2 Motivation

1.2.1 Mechanical Strength Testing

Mechanical testing of tissues provides a baseline strength that may be used to assess weld strengths. Heating the tissues both in a steady-state waterbath and with repetitive laser pulses will show how temperature affects overall tensile strength. Given that heating causes several changes to occur in the tissue, it is important to quantify their effects on tissue strength. A significant change in strength after exposure to laser light could lead to an entirely different evaluation of weld strength. If the mechanical strength of an exposed tissue is significantly less than that of unexposed tissue, welding strength comparisons will change. These mechanical tests are vital to the understanding of the interaction between tissue and heat, and its effects on tissue strength.

1.2.2 Thermal Characterization

Laser welding is a thermal process: localized heating of two tissue surfaces under pressure can cause a bond to occur between them. Welding will not occur without localized heating of the tissue, nor will it occur without pressure to ensure good tissue contact.

To achieve reliable welds, the process of heating with laser irradiation must be thoroughly understood. The two main components responsible for heating are the optical characteristics of the tissue itself, and the laser parameters used to weld.

1.2.3 Optical Characteristics of Tissues

Biological tissue has several optical properties, the most important for heating being absorption. However, plain tissue is rather transparent at 800 nm, with a transmission of more than 90% *. Thus photochemically active dyes such as indocynanine green (ICG) are used to create a confined absorbing layer on the tissue surface. When laser light is applied, the heat it creates is confined to this layer, usually 25–100 μm thick. This creates a small zone of rapid heating, and little thermal damage to the surrounding tissue.

The confined area of heating is also known as the optical zone. The optical zone in tissue, as defined by Jacques, is the depth in the tissue where the fluence has dropped to 35% of the original laser radiance [5]. To achieve strong welds and minimize thermal damage, thermal diffusion must be slow enough as to not leave the optical zone during the laser pulse. This concept is otherwise known as thermal confinement. It is achieved by using laser pulse durations less than d^2/κ, where d is the thickness of the absorbing layer, and κ is the thermal diffusivity of the tissue. Thermal confinement must be maintained to control collateral tissue damage, and therefore create a strong weld with little disturbance to the surrounding tissue structure.

There is currently concern for exactly how thick the absorbing layer is in each type of tissue used for welding. However, previous results indicate that the absorbing layers are between 25 and 100 μm, making the 5 ms pulse length used for this study well within the thermal confinement time of 4–64 ms.

The time for which a weld is heated effects the weld strength: this leads to a relationship between time, temperature, and weld strength. If steady-state welds are created by varying temperature and time separately, the time and temperature required to obtain

*Transmission was measured on unstained samples of porcine aorta (thickness 1–2 mm) and intestine (thickness 300–500 μm) at a wavelength of 808 nm.

an optimum weld can be found for each type of weld tissue. These waterbath welds will provide a thermal basis for the strongest welds possible. Lastly, thickness of the particular tissue being used must be taken into consideration. The thickness can change the amount of laser irradiation needed to heat the stained layer evenly. Thinner tissues such as intestine and carotid artery need less irradiation than aorta in order to achieve the same result.

1.2.4 Laser Parameters for Welding

Several laser parameters affect the amount of heat applied to the weld site during welding: radiant exposure, pulse length, number of pulses, and pulse repetition rate. Thus, a thorough investigation must be done to optimize each parameter, and find the right combination to obtain the best weld. Also, each of these welds must be repeated several times to determine individual weld variability.

1.2.5 Welding Mechanism

The actual mechanism that causes welding between two tissue samples remains to be identified. Biological tissues consist of several proteins that could be factors in the welding process, but the particular constituents responsible and their variations in content from tissue to tissue need to be investigated. Studies of mechanical strength, thermal characterization, and steady-state welding will lead to a better understanding of the mechanism for each tissue type. This understanding of the actual welding mechanism is the key to strong, reliable, and consistent welds without excessive amounts of collateral thermal damage to surrounding tissues.

1.3 Background

1.3.1 Protein Denaturation and Coagulation

When tissue is exposed to heat, the first major change is denaturation of tissue proteins, starting with collagen. Dew *et al.* describes this first event as denaturation or pre-collagen shrinkage, which can start as low as 45°C, and is most evident between 60 and 70°C [4]. Denaturation is a structural change in any biopolymer which destroys the native active configuration [6]. This change can be caused by heat, pH changes, or chemical agents that break or form new bonds. For example, two separate collagen proteins might denature and then bind to one another, in a process otherwise known as coagulation [6]. Extending this concept to two tissue surfaces, then a weld could occur when heat is applied and proteins from both surfaces coagulate together.

1.3.2 Thermal Damage as a Rate Process

Henriques *et al.* was one of the first groups to perform an in depth study of thermal injury, and model it as a rate process with respect to time and temperature [7]. Given the temperature and time of exposure, they were able to predict the extent of thermal damage that occurred to the tissue. Agah *et al.* used this information to develop a numerical model of thermal damage based on protein denaturation kinetics [8]. This theoretical model is derived from an Arrhenius equation that is typical of most chemical or physical processes. The two key factors used in this model to relate damage to time and temperature are A and ΔE. A is known as a frequency factor, and has units of s^{-1}, relating the damage to time, and ΔE is the activation energy in Joules/mole, relating damage to temperature and the tissue itself. Values for these two factors can be determined experimentally for a given tissue, therefore creating a first-order reaction rate process for thermal damage. Pearce *et al.* created two sets of damage coefficients to distinguish between collagen damage and smooth muscle damage. From the Arrhenius model, they also created a numerical model for thermal damage caused by laser irradiation [9].

Several simplifying assumptions were made in both of these models. First, a constant temperature exposure was assumed for a specified amount of time. Second, the Arrhenius equation model was simplified by creating a point of threshold damage where approximately 63% of the tissue constituent of interest has been damaged in the area heated. Lastly, the damage rate does indeed approximate first order kinetics.

The determination of the damage parameters A and ΔE in these studies had large variations. This is mostly due to difficulty in accurately pinpointing a threshold for damage. However, several studies have found a relation between damage rates, collagen content, and denaturation point [10–12]. Collagen has the lowest denaturation point of any protein constituent of tissue, and therefore it is the first to undergo a thermal change.

1.3.3 Tissue Constituents: Collagen and Elastin

All biological tissues have several components, but a good portion of them are collagen and elastin proteins. Collagen is an extracellular protein responsible for the strength and flexibility of most connective tissues. Collagen comprises 25–30% of all the proteins in biological tissue [6]. The amount of collagen in each type of tissue may vary greatly, even within a given vessel or intestinal section. Harkness reported that the collagen content of aorta varied linearly with distance from the heart, with approximately 25% at the start of the aorta to about 75% at the division to the iliac arteries [13]. Collagen is the main cause of protein denaturation, and has been linked to tissue welding by several studies. Bass *et al.* found an absence of helical structure in collagen after laser exposure. Thus denaturation had occurred, causing a change in the collagen structure, and a reformation of new collagen matrices [14].

During the collagen denaturation process, the fibrils shrink and the tissue itself contracts. Gorish *et al.* observed heat-induced spontaneous contraction of blood vessels during laser irradiation. In evaluating temperature dependence on contraction of the blood vessels, they found that the temperature threshold for contraction was between 70 and 75°C. Histological examination revealed that this contraction correlated with the

denaturation of collagen fibrils [15].

Elastin is the other major constituent of many connective tissues. Elastin is a structural protein that is the main component of elastic fibers such as skin, ligament, and arterial walls [6]. Harkness found aortic elastin content to be highest near the start of the aorta, and decreases linearly with distance from the heart [13]. Elastin is insoluble, hydrophobic, and highly crosslinked, making it resistant to denaturation. Elastin is stable above 100°C, and therefore does not appear to contribute to welding in the same manner as collagen. However, the overall welding mechanism is still not fully understood, and therefore elastin could play a role when welding tissues with high elastin contents.

1.3.4 Mechanical Properties of Biological Tissues

Most biological connective tissue consists of two main components: protein fibers (elastin and collagen), and an amorphous matrix in which these fibers are embedded [16]. Each constituent has different mechanical properties, and each plays a different role in strength and elasticity. Harkness *et al.* found that collagen forms the fibrous structure and gives tissue its mechanical strength. This strength is highly dependent upon covalent cross links between collagen molecules. These bonds can easily be altered by mild reagents. Reagents that reduce the pH of a collagen structure can cause a marked decrease in mechanical strength, reversible upon return to a neutral pH. Thus, the mechanical properties are highly dependent on details of the tissue's microstructure, specifically on the state of certain molecular links [17]. Minns *et al.* determined the mechanical effects produced by isolating each component in human tendon, aorta, and bovine ligamentum nuchae. Removal of the ground substance with EDTA and α-amylase induced a decrease in strength in all three tissues, leading to a connection between the ground substance and the structure of the fibrous proteins. Removal of both ground substance and collagen with formic acid produced a dramatic decrease in strength in both aorta and nuchal ligament. Therefore, ground substance and collagen were the significant strength components, while elastin was the component responsible for flexibility [16].

1.4 History of Laser Welding

Attempts have been made to weld biological tissues with argon, CO_2, Nd:YAG, THC:YAG, and IR pulsed and CW diode lasers. White *et al.* found that the argon laser was successful for several forms of anastomoses including venotomies, arteriotomies, and arteriovenous fistulas. They found argon laser fusion of both small and large vessels to be comparable in strength to suture repairs, with an absence of the foreign body reaction. However, argon laser welding appears to involve several mechanisms including apposition of denatured collagen and elastin, and coagulation of platelets and fibrin [18,19]. Fujitani *et al.* described argon laser welding as fusion created by a physiobiochemical bond created by annealing collagen at temperatures between 43 and 48°C [20]. In contrast, Martinot *et al.* performed end-to-end carotid anastomoses with an argon laser, claiming the mechanism to be collagen denaturation at a temperature of 77°C [2]. These studies show argon laser welding is successful for a variety of situations, but are unable to pinpoint the exact fusing mechanism.

Welding with CO_2 lasers has been performed successfully in several studies [21–23]. Badeau *et al.* and Serure *et al.* produced microvascular anastomoses with a CO_2 laser as a result of collagen denaturation between 80 and 120°C [21,22]. All these studies reported a 10–20% chance of aneurysm post-operatively due to tissue necrosis from the intense heat created by the CO_2 laser because of its very small 10 μm penetration depth. More recently, Shenfeld *et al.* found a 55°C optimum for low power CO_2 laser welding of rat urinary bladders, as measured by fiber optic radiometry [24]. They proposed the mechanism to be structural changes in tissue matrix proteins that form crosslinks. Again, the mechanism remains unclear.

Several other successful welding studies have used varying types of YAG lasers including THC:YAG and Nd:YAG. Oz *et al.* compared laser welding to sutured closure for biliary tissue both *in vitro* and *in vivo*. They found welding to be successful, with less scarring and inflammation than sutured closures [3,25]. Kuramoto *et al.* reported

the first sutureless anastomosis of the colon with an Nd:YAG laser and indigo ink, yielding accelerated healing over the sutured controls [26]. Both studies claim laser welding to be a subjective process, with great dependence on operator expertise. Also, several mechanisms may be involved, that may differ from tissue to tissue, and from laser to laser.

Diode and alexandrite lasers using infrared wavelengths and indocynanine green (ICG) staining are other current methods of laser tissue welding. DeCoste *et al.* performed successful skin closures with an alexandrite laser at 780 nm and determined a range of irradiances for optimum welding. They also found an inverse relationship between irradiance and staining concentration in the optimal welding range [1]. Tang *et al.* performed direct carotid end-to-end laser anastomosis with a CW 830 nm diode laser and no chromophore. They discovered laser treatment sped up the operating time by almost 50%, as well as healing time due to less foreign body interaction. The advantages of the diode laser include its small size and lack of an external cooling system supply [27]. Both studies determined further optimization was necessary for this type of laser welding to be clinically acceptable.

For the welding in this study, we have chosen to use a pulsed diode infrared laser, based upon its many advantages in size and weight. Depositing the laser light in pulses guarantees thermal confinement, since the heat from each pulse stays in the optical zone. The 808 nm infrared wavelength is poorly absorbed by tissue, but strongly absorbed by ICG, therefore creating a confined area of heating on the tissue surface, where it is most needed for welding. Also, pulsed laser light allows heat to be applied in discrete doses (pulses) that may reduce operator-to-operator variability.

Chapter 2

Materials and Methods

2.1 Tissue Preparation

All tissues except the elastin biomaterial were obtained at Carlton Packing Co., Carlton, OR. They were freshly cut and placed on ice. Each tissue was then frozen at -10°C until thawed for use. All tissues were handled with latex gloves and surgical equipment.

2.1.1 Porcine Aorta

Porcine aorta came in sections approximately 50 cm in length, and were thawed by placing the freezer bag directly in a beaker of room temperature tap water. Once thawed, the aorta is removed from the bag, rinsed lightly with cool water, and split open lengthwise with surgical scissors. Rectangular sections about 3–5 cm were cut with scissors, and then used in the dog bone cutting mold (see Figure 2.1). This dog bone shaped mold is typical of mechanical testing shapes, and makes each sample have approximately the same surface area, a critical parameter in strength testing. The thinner center area provides more accurate testing by ensuring that the sample will fail in the center first, instead of failing at the grips. The cut samples were stored in gauze soaked with 0.9% NaCl, in order to prevent drying.

2.1.2 Porcine Intestine

The intestine usually came fresh in about 8 m lengths, and were cut in 10 cm sections before freezing in individual freezer bags. They were thawed in the same manner as the

aorta, but rinsed more thoroughly. The intestine was split open, and the inside wiped clean with gauze. Each section was cut in the same manner as the aorta, and then cut with the mold. The samples were stored in saline soaked gauze until use.

2.1.3 Heterograft

Porcine carotid heterografts are carotid arteries that were treated to remove all the adventia, and just leave the elastin core of the vessel. The carotid arteries are brought in either fresh or thawed, and individually cleaned. Excess fat is removed with scissors, and groups of 5 arteries are placed in 200 ml of 0.5M sodium hydroxide (NaOH), and sonicated for 45 minutes at 70°C. This step removes all tissue constituents but the elastin core. The heterografts are then placed in a room temperature deionized waterbath for 30 minutes, then boiled in deionized water for 30 minutes, in order to remove the NaOH, and disinfect the vessels. Each heterograft was prepared for testing by sectioning into 2 cm sections. These vessels are about 5 mm in diameter, and very thin, making them difficult to split like the aorta and intestine. Thus, all heterograft tests were done with the flattened vessel, resulting in twice the thickness, but only one surface was used for the welding experiments.

2.1.4 Elastin Biomaterial

The biomaterial used in the thermal characterization experiments was produced in the laboratory, and is an emulsion of elastin and fibrin in a phosphate buffered saline solution polymerized by thrombin to create a soft tissue-like structure. The elastin and fibrin structure give the biomaterial its strength. This material is currently in its early stages of development, and is similar in structure to the elastin heterografts, but not nearly as strong and durable. Thus, I only used the biomaterial in the thermal characterization studies, instead of the elastin heterografts. The heterografts were not tested since their elastin content is very high, and the denaturation point of elastin is above 100°C. The biomaterial was stored in refrigerated 33% ethanol, placed in 0.9% saline solution to warm to room temperature, then removed, cut with the mold, and placed back in saline

until tested.

2.2 Indocynanine Green Preparation and Staining Process

For the laser strength tests and for laser welding experiments, the tissues were stained with different concentrations of Indocynanine Green (ICG). ICG is stored under vacuum in a dry container to keep it from becoming moist. For each concentration, the correct amount of ICG powder was measured out and added to 1 ml of deionized water in a small test tube. The test tube is vortexed for 2–3 minutes to completely dissolve the ICG and create a clean green solution with no ICG granules. To stain the tissue, a large section is used before the tissue is cut into smaller pieces for welding to ensure one even stain for each set of experiments. The tissue is laid flat on a cutting board, and the stain is dropped on with a disposable pipette, left for the appropriate staining time (usually 5 minutes), and dabbed off with a tissue. Staining is usually performed on the smoothest side of the tissue; for aorta, the intimal layer (inside), and for intestine and heterograft, the serosal layer (outside). The stained tissue is then sectioned for testing or welding.

2.3 Yield Strength Tests

Yield strength tests were performed using the Chatillion Vitrodyne V1000 universal tester. This tester consists of a computer-controlled motorized actuator in a vertical position, and variable strength load cells*. The load cell was calibrated according to the manufacturer's instructions at the beginning of each day, or when a new load cell is used. The prepared samples were placed in the tester grips, which consisted of two sliding metal plates backed with plastic screws to secure the sample (Figures 2.2 and 2.3). A strength, or ramp test was performed by pulling on the sample at a constant speed (200 μm/sec), and measuring the tension exerted by the sample. This test was

*The load cells have different peak strength capacities, and their accuracy is 0.05% of peak capacity. Different load cells are chosen depending on the strength of the material, and the desired accuracy of the test.

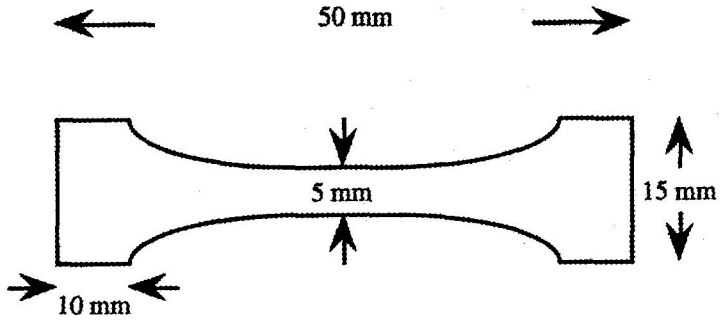

Figure 2.1: Dog bone shaped die mold used to section the aorta, intestine, and biomaterial samples for mechanical testing.

repeated five times for each tissue type.

2.3.1 Heated Yield Strength Tests

To measure the effect of temperature on tensile strength, the tissue was first heated in 500 ml of water. A small stirring bar in the bottom of the beaker kept the temperature uniform. Samples were immersed in the 80°C water for 5 minutes, removed, and then cooled in room temperature saline. The same ramp test was performed as above.

2.3.2 Laser Yield Strength Tests

The effects repetitive laser pulsing on the tensile strength of the tissue was also measured. A pulsed diode laser (Star Medical Technologies) that operates in a wavelength range of 790–810 nm, with variable pulse durations, energies, and repetition rates was used. A handpiece with three different copper coated condensers allow spot sizes of 9, 16, and 36 mm^2 with 3×3, 4×4, and 6×6 mm square outputs. Both porcine intestine and aorta were cut to shape with the die mold, and stained for 5 minutes with 6.5 mM indocynanine green solution. The samples were placed in the tester grips, and the 6×6 condenser tip placed 2–3 mm from the sample to irradiate the center of the dog bone

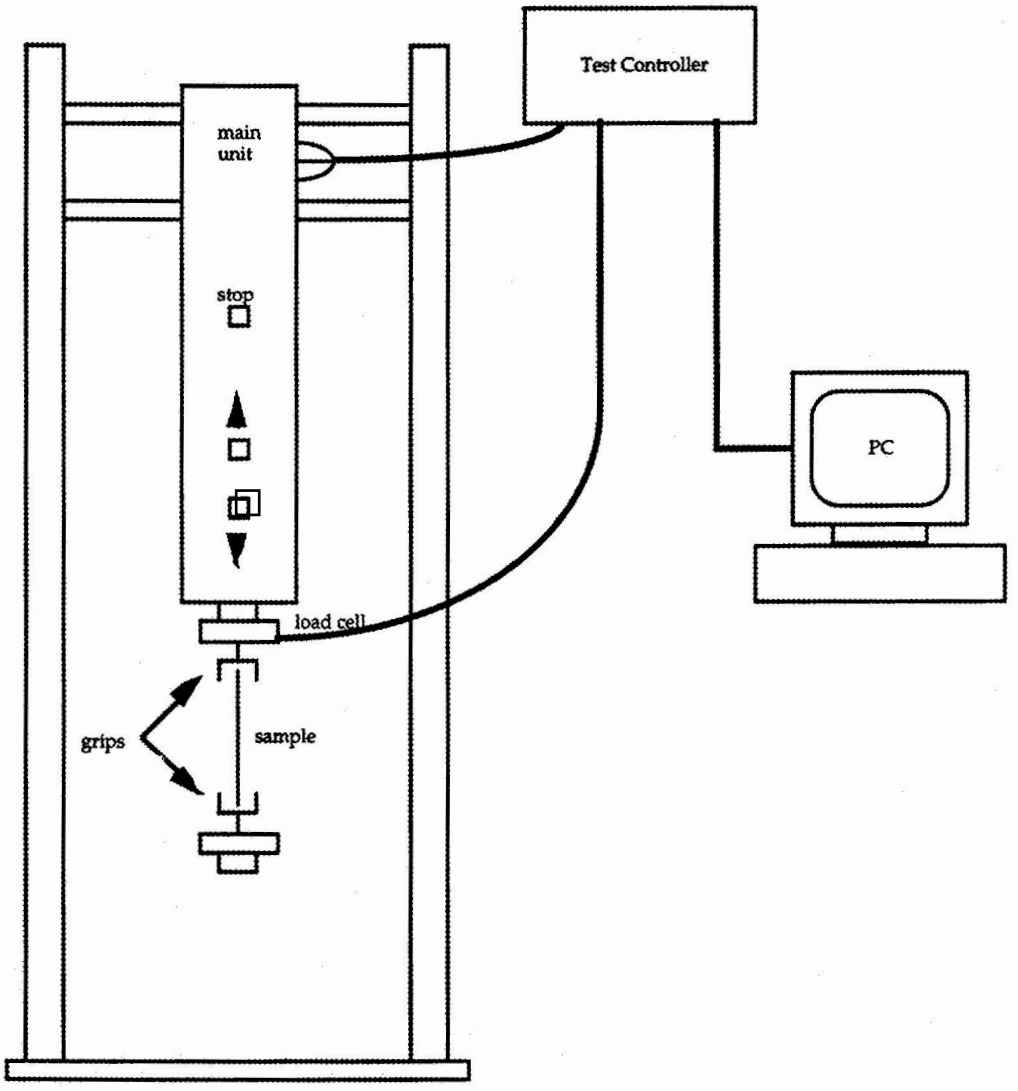

Figure 2.2: Chatillion Vitrodyne V1000 Universal Tester Setup. The tester can be mounted vertical or horizontal, and has an arm to hold the bottom grip stationary, while the force is measured at the top grip. This allows for submersion of the sample during testing.

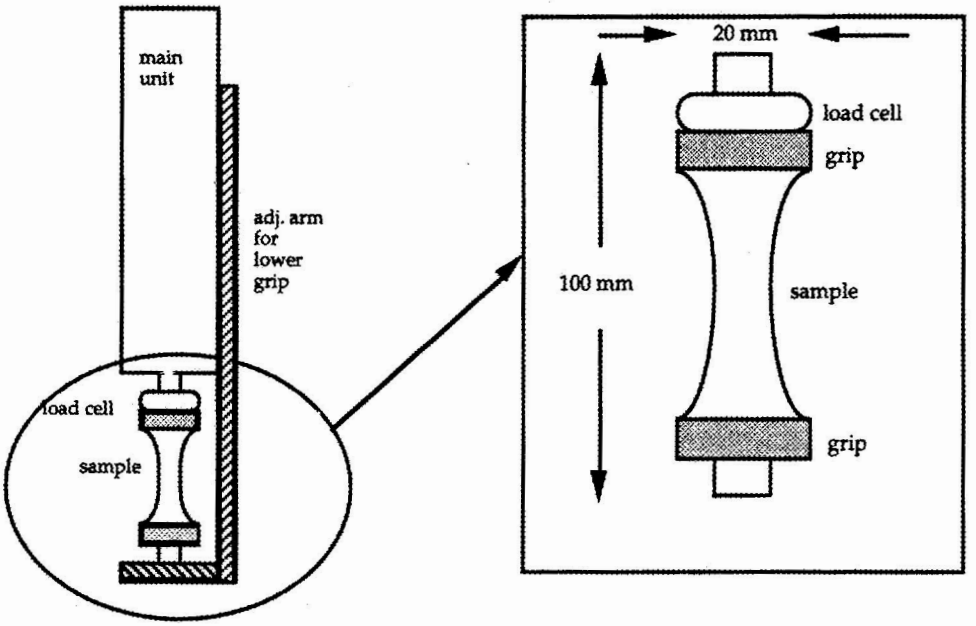

Figure 2.3: Tissue shape and tester grips (side view), showing the bottom grip arm, and the sample stretched between the two grips. Also shown is a closer view of the sample, grips, and load cell.

shape perpendicularly. Five to twenty pulses were fired at the sample with a radiant exposure of 75 mJ/mm^2, a repetition rate of 1 Hz, and a pulse length of 5 ms. The same ramp test as above was then performed, and the yield strength recorded.

2.4 Thermal Characterization

2.4.1 Waterbath Tests

One thermal characteristic of tissues is the denaturation and coagulation of tissue proteins that cause tissue to contract or shrink. The following set of experiments measured the rate of contraction for varying temperatures. The tissue preparation was the same as for the strength tests, but the type of test differed. I performed a creep, or pull-to-force test where each sample was pulled to about 10% of yield strength. This force is maintained and the length is monitored over time.

The proportional gain, integral gain, and integral clipping must be set so the tester will pull the sample at a constant force without oscillation. The precise settings depend on the length of sample and its elasticity. The following table shows the values used for each type of material (Table 2.1). These were obtained by setting the integral gain to 1 and the integral clipping to 100, and adjusting the proportional gain to be as high as possible without causing oscillation. Several samples were tested to optimize these gain values.

Table 2.1: Creep test parameters for waterbath tests (unitless).

Tissue Type	Proportional Gain	Integral Gain	Integral Clipping
intestine	400	1	100
aorta	1200	1	100
biomaterial	700	1	100

The sample was placed in the grips, a large beaker was placed underneath, and raised up over the sample (The tester configuration enabled this to be done easily. See

Figure 2.4). The sample was pulled to force, heated water added to the beaker, and the change in length monitored at 5 samples/second. The temperature of the waterbath was measured with a thermocouple during the peak of tissue contraction for each test. This test was repeated for temperatures ranging from 50–90°C for each tissue type. I normalized the exponential curve created by a plot of position versus time. This was accomplished by the following equation:

$$x_{norm} = \frac{x - x_{end}}{x_{start} - x_{end}} \tag{2.1}$$

The above normalization produces a decaying exponential with a maximum equal to 1.0 and a minimum equal to 0.0. This normalized decaying exponential curve has an equation of the form $e^{-\alpha t}$, with the rate of the exponential decay corresponding to the value of α. I produced a plot of $-\ln(x_{norm})$ versus time, and used a linear regression to determine the value of α, the rate of contraction, given by:

$$\alpha = \frac{-\ln(x_{norm})}{t} \tag{2.2}$$

Other trends analyzed include the change in length after the heat was applied:

$$\epsilon = \frac{x_{end} - x_{start}}{x_{start}} \tag{2.3}$$

The variable ϵ is a strain ratio, where the ratio is positive for increases in length, and negative for a decrease in length. The starting and ending lengths include the addition of about 4 cm for the initial length of the sample between the grips.

2.4.2 Laser Tests

The laser contraction experimental set-up was similar to the waterbath setup. Sample preparation was the same as for the laser yield strength tests. Instead of the waterbath beaker, the Star pulsed diode laser was used. The pulse length was fixed at 5 ms, and using the 6×6 condenser, the radiant exposures varied from 27–75 mJ/mm^2 and the repetition rate from 0.5–3 Hz. First, the sample was stained with 6.5 mM ICG for

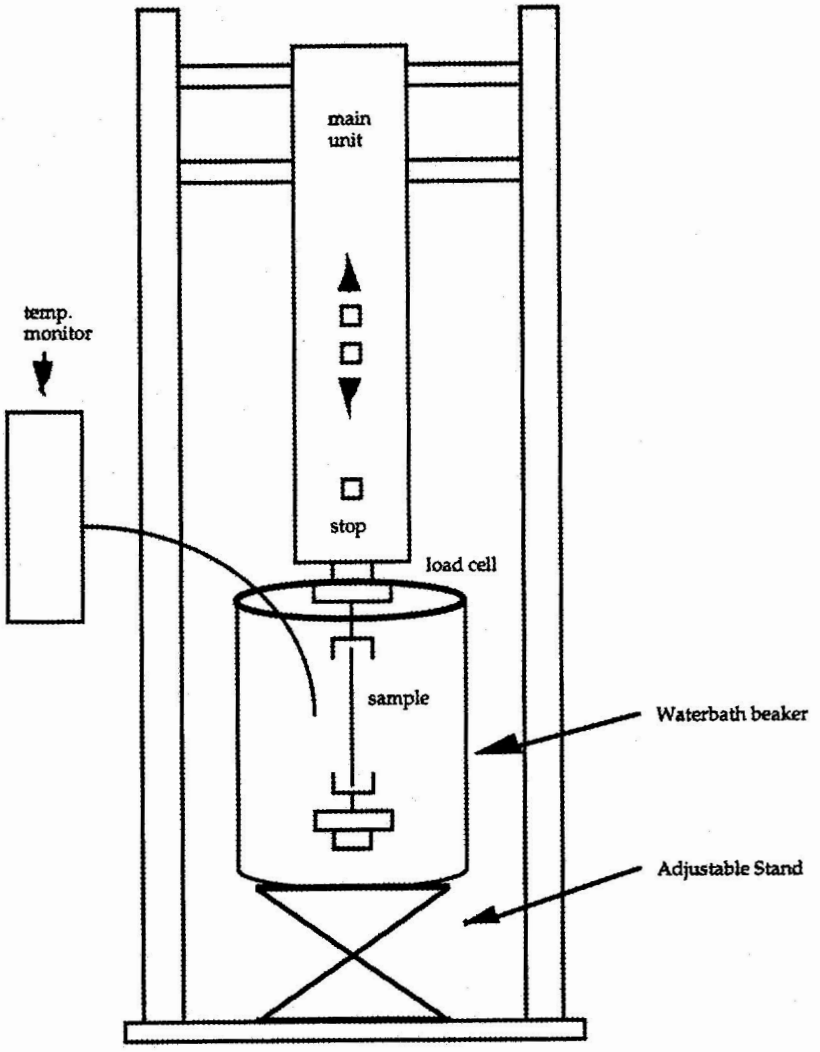

Figure 2.4: Universal tester setup with hot waterbath used for the thermal contraction experiments.

5 minutes, then placed in the tester grips, and pulled to 10% of yield strength. The laser condenser tip was placed 2–3 mm from the sample, and a open port of a 6 inch integrating sphere (Labsphere) was positioned approximately 1 cm away on the other side of the sample (see Figure 2.5).

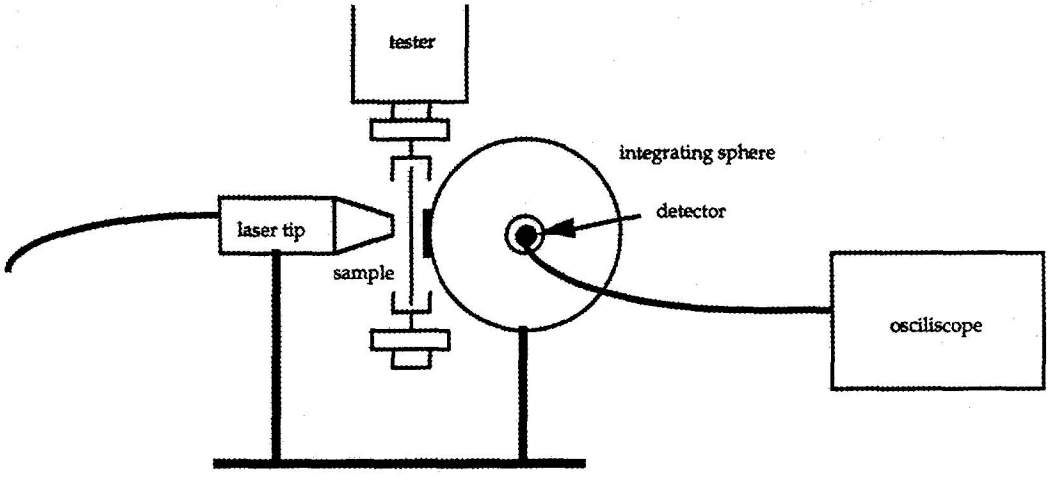

Figure 2.5: Universal tester setup with laser condenser tip and integrating sphere to measure laser induced contraction and transmission simultanuously.

Since ICG stained tissue often bleaches from green to orange with repetitive pulses, transmission was measured through the sample with each laser pulse. Transmission measurement during pulses was accomplished with the integrating sphere, a silicon photodiode detector, and an osciliscope. The detector was placed in a port 90° from the sample, with an internal baffle preventing direct laser irradiation of the detector. The change in voltage from the detector was recorded after each pulse. The change in voltage for unstained tissue was used as a reference for maximum transmission. Transmission in stained tissue is calculated from the voltage of unstained and stained tissue:

$$T_s = \frac{V_s}{V_u} \tag{2.4}$$

Where $\mathcal{T}_s$ is transmission, V_s is the voltage for stained tissue, and V_u is the voltage for unstained tissue. As the pulses were fired on the sample, the tester monitored the change in overall length of the sample with respect to time, and plots of length vs. time were produced.

2.5 Waterbath Tissue Welding

A series of waterbath welding experiments were performed using an Equatherm waterbath that holds temperatures constant within one degree. Five types of waterbath welds were attempted: aorta to aorta, intestine to intestine, heterograft to heterograft, aorta to heterograft, and intestine to heterograft. The intestine and aorta were die cut, and then cut in half. One half was flipped over, and then overlapped with the other piece about 5 mm. This enabled all welds to have approximately the same surface area of 25 mm^2. The heterografts were not die cut because they are roughly the same size as the die center itself. They were cut into about 2 cm strips, and overlapped approximately 5 mm with each other, or with the aorta or intestine.

Waterbath welding has been shown to require a fair amount of pressure for the two tissues to form a bond [28]. The overlapping tissues were sandwiched between 2×2 cm glass slides with 220 grit sandpaper in between the tissue and glass to hold the weld site in place. A small binder clip was used to apply approximately 800 N/cm^2 pressure to the weld site (see Figure 2.6). Welds were immersed at temperatures of 60–80°C, for 3, 5, 7, 10, and 15 minutes, then removed from the waterbath and placed in room temperature saline to cool. The clips and glass slides are removed, and the weld placed in the tester grips. A ramp test was performed at 200 $\mu m/s$, and the yield strength of the weld was recorded.

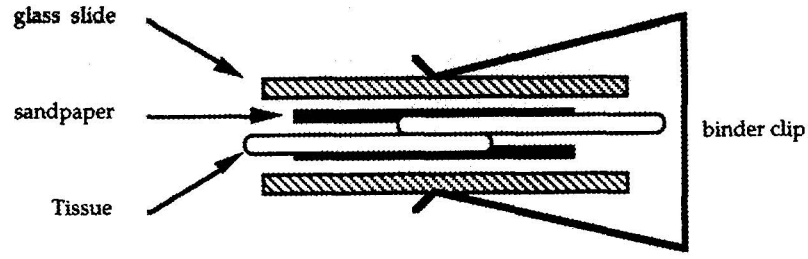

Figure 2.6: Waterbath welding grips made with two glass slides, sandpaper, and a binder clip.

2.6 Laser Tissue Welding

The laser parameters (radiant exposure, pulse length, pulse number, and repetition rate), ICG staining concentration, and staining time are all ways in which to vary the laser welding process. From previous attempts at laser welding, I found that the most important parameters were radiant exposure, staining concentration, and number of pulses. Given that all staining depths are between 25–100 μm, thermal confinement is maintained for all pulse lengths available with this laser, and so I chose the longest time available, 5 ms. Previous welding also demonstrated that higher repetition rates were more effective in creating uniform heating, so I chose the fastest possible repetition rate with the Star laser: hand pulsing at about 2–4 Hz. Lastly, staining times over 5 minutes did not seem to produce darker stains, so I stayed with 5 minutes. Therefore, I narrowed the scope of experimental parameters by keeping pulse length constant at 5 ms, rep rate between 2–4 Hz, and using two radiant exposures, two staining concentrations for 5 minutes, and 5 to 30 pulses.

The setup for laser welding consists of two overlapping pieces of tissue sandwiched between a glass slide and a 1 inch styrofoam layer giving roughly the same welding area as in the waterbath welds. I found the styrofoam layer helped keep the tissues stationary while under pressure (Figure 2.7). The sample was placed on a small digital scale, and

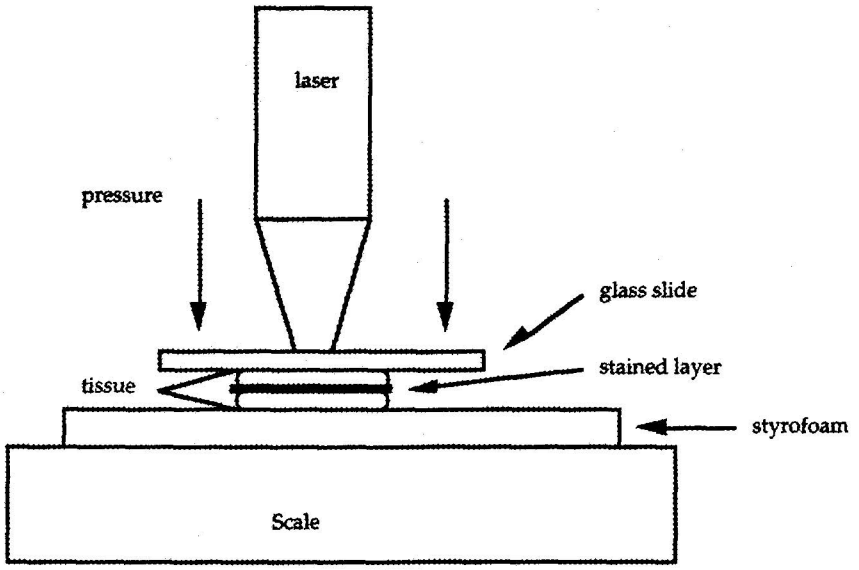

Figure 2.7: Laser welding setup. Pressure is applied by hand, and monitored with the scale. The styrofoam layer helps keep the tissues stationary.

the laser condenser placed on top. A pressure of 2 kg was applied by hand, and monitored with the scale. Once the sample was irradiated, it was placed in the tester grips for the same tensile strength test as the waterbath welds, and the weld yield strength recorded.

Chapter 3

Results

3.1 Yield Strength Tests

The yield strength of porcine intestine, aorta, and heterograft varied greatly from sample to sample. Though the samples had less than 10% variation in size, they had 50% variation in thickness, a key factor in the measurement of overall yield strength. The yield strength is also dependent upon whether the section is cut longitudinally or radially. The aorta samples showed this most dramatically, with a yield strength for a radial section 2 to 3 times stronger than a longitudinal section. A typical curve for a tensile strength test is shown in Figure 3.1. The load increased linearly until the sample ruptured. The average values and their variances are given in Table 3.1.

Table 3.1: Average yield strength for porcine aorta, intestine, and heterograft. Each tissue has a 25–30% variation.

Tissue	number of samples	average strength (N/mm^2)
intestine	5	1.4 ± 0.3
aorta (lengthwise)	5	1.5 ± 0.6
aorta (radial)	1	$4.8 \pm 0^*$
heterograft	5	0.3 ± 0.1

*only one sample tested

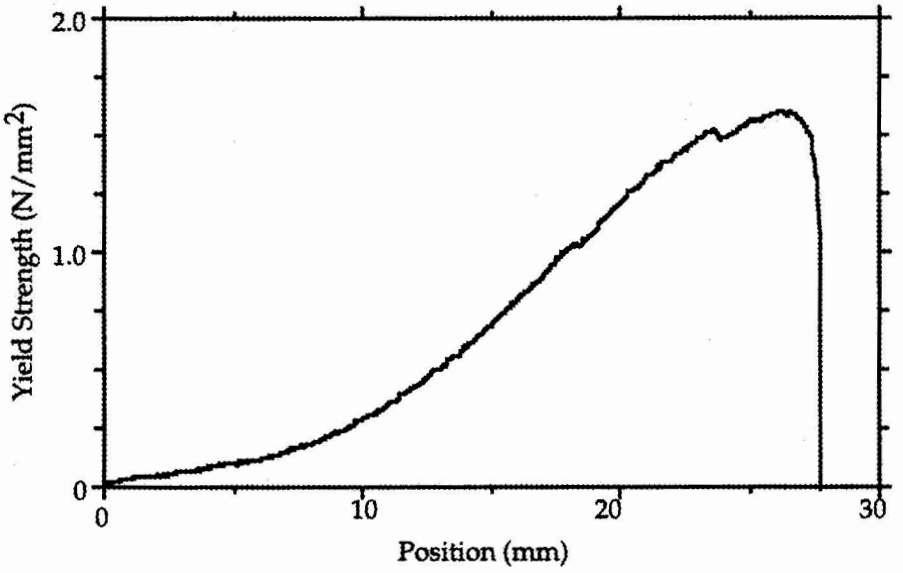

Figure 3.1: A typical curve for a yield strength test on a longitudinal intestine tissue sample cut with the die mold. The intestine failed at about $1.6\,\mathrm{N/mm^2}$.

3.1.1 Heated Yield Strength Tests

Tissue samples preheated in the waterbath did not lose any of their original strength. The average yield strength for all tissues tested was within 20% of the average for unheated strength. This average is within typical yield strength variations due to differences in size and thickness.

3.1.2 Laser Yield Strength Tests

Intestinal tissue samples exposed to repetitive laser pulses decreased in yield strength. This trend can be seen in Figure 3.2 where the strongest sample had no laser irradiation, and the weakest had 25 pulsed exposures. The average yield for the pulsed samples is $1.1 \pm 0.3\,\mathrm{N/mm^2}$, or about 75% of unirradiated yield strength of $1.4 \pm 0.3\,\mathrm{N/mm^2}$.

3.2 Thermal Characterization

3.2.1 Waterbath Tests

The exposure of both porcine intestine and aorta to heat caused several changes, most notably a contraction of the tissue itself. Other changes included color (usually from light pink to white), texture (smooth to coarse), and thickness (from thinner to thicker).

Typical contraction curves for porcine intestine and aorta are shown in Figures 3.3 and 3.4. When exposed to heat, intestine shrank with a single distinct exponential decay. The aorta initially shrank rapidly in the first 10 seconds, and then somewhat slower over the next 100–150 seconds.

The heated waterbath tests for contraction were performed on several samples of elastin biomaterial, with entirely different results. The biomaterial contains no collagen, and therefore does not contract when exposed to heat. Instead, the biomaterial weakened when exposed to the heated water as evidenced by the increase in length after immersion in warm water. The tester attempts to maintain a constant force, while the strength of the biomaterial weakens, resulting in an increase in length. A typical curve for the biomaterial is shown in Figure 3.5.

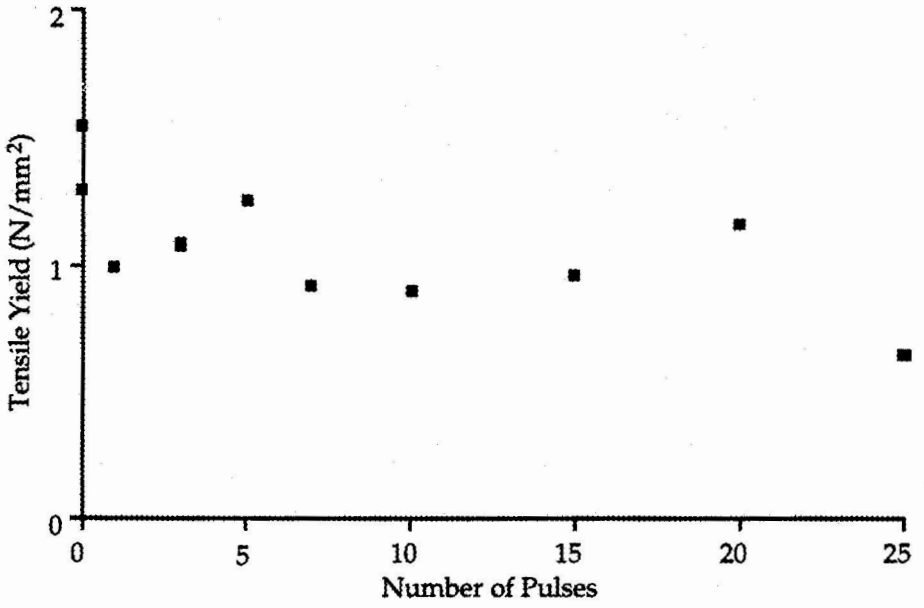

Figure 3.2: Tensile yield stress of intestine exposed to multiple laser pulses. Strength decreases slightly with increasing pulse number. (One sample per point. Initial cross section: 2.5 mm^2)

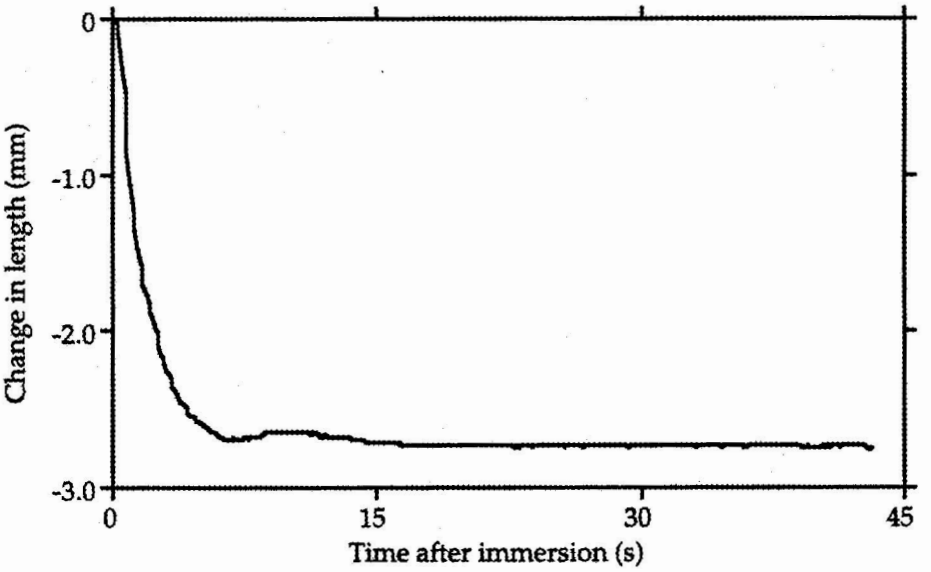

Figure 3.3: Porcine intestine shrinkage at 85°C. Prior to immersion at time zero the intestine was pulled to 10% of yield strength. One exponential decay can be seen. The cross sectional area of the sample was 2.5 mm^2.

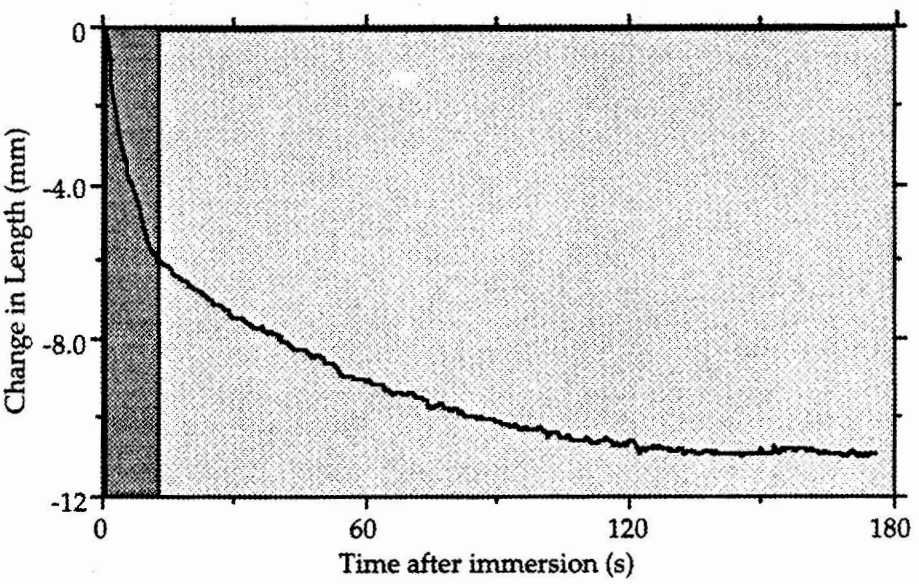

Figure 3.4: Porcine aorta shrinkage at 89°C. Prior to immersion at time zero the aorta was pulled to 10% of yield strength. Two exponential decay rates are evident. The cross sectional area of the sample was $5\,mm^2$.

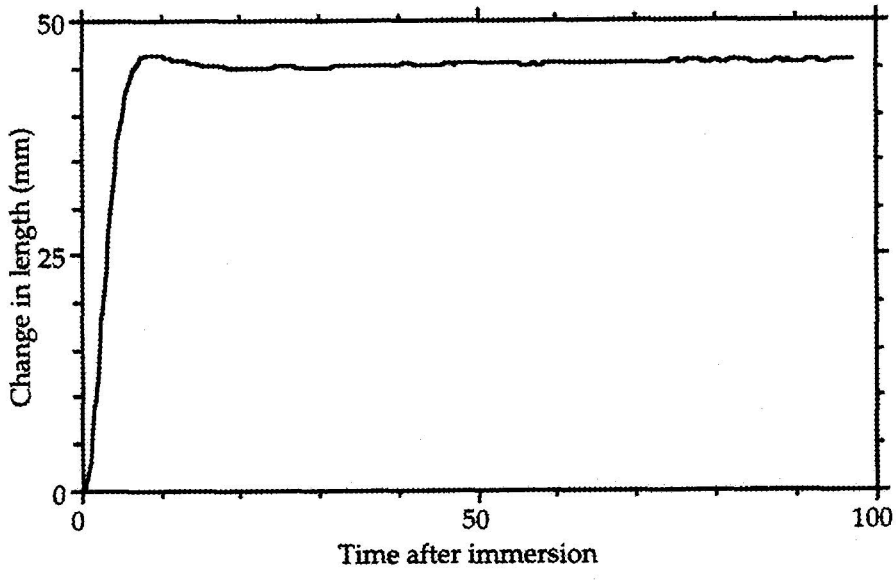

Figure 3.5: Typical elongation of elastin biomaterial following immersion in a heated waterbath at 91°C pulled to 10% yield, or 0.2 N. The cross sectional area was 5 mm^2. Length increases when the water is added, and then stays constant once the biomaterial reaches the water temperature.

I hypothesized that the contraction for intestine and aorta and the lengthening of the biomaterial were exponential, and found exponential rates of contraction and strain values following the data manipulation method described in section 2.4.1. Figures 3.6 and 3.7 show a linear regression for two intestine samples and two aorta samples, respectively. I attempted to match the most linear portion of the graph in order to obtain the best fit. This section always started at the beginning of the curve, and ended with variation as x_{norm} approached zero. The deviation from linear occurs at this point because $\ln(x_{norm})$ approaches infinity as x_{norm} approaches zero. The linear regression gave different values of α for each sample, including one for each intestine and biomaterial sample, and two for each aorta sample, corresponding to the two areas of contraction. Strain ratios (change in length over original length) for each sample were also produced.

Figure 3.8 shows the coefficient of contraction α_1, and the strain ϵ for intestine as functions of temperature. In all, 19 samples were tested over a temperature range of 70–90°C. The rate of contraction for intestine is independent of temperature, while strain has a threshold at about 77°C. The average contraction above and below 77°C is:

$$\alpha_1 = 0.6 \pm 0.1\,\mathrm{s}^{-1}$$

While the average strain is:

$$\epsilon = -0.01 \pm 0.005 \text{ below } 77°\mathrm{C}$$
$$\epsilon = -0.05 \pm 0.03 \text{ above } 77°\mathrm{C}$$

Figure 3.9 shows the first and second contraction coefficients for aorta versus temperature. The initial rate occurs during the first 10 seconds of immersion, has a threshold temperature of 65°C, with an average value of $\alpha_1 = 0.07 \pm 0.03(s^{-1})$. The second contraction rate α_2 is almost constant with temperature, with a possibly increasing slope. The average value of ϵ is linear with a slope of -0.04 ± 0.004 (1/°C) and does not exhibit a threshold effect like intestine does (Figure 3.10).

The weakening of the biomaterial is linear with temperature, with both the rate and strain increasing as temperature rises (Figure 3.11). The biomaterial also did not return

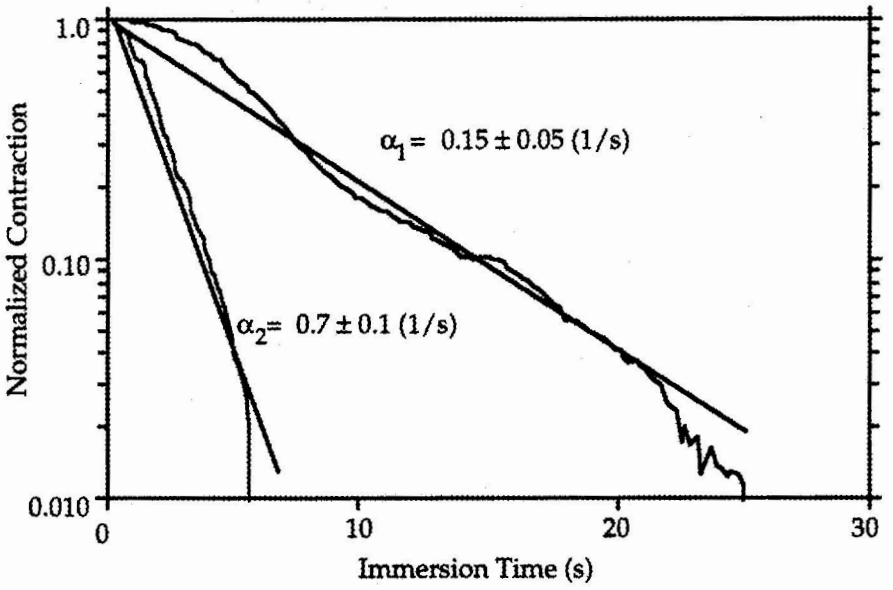

Figure 3.6: Plot of normalized position versus time on a semilog scale for two intestine samples in a heated waterbath at 79°C (α_1 bottom line) and 80°C (α_1 top line) pulled to 10% of yield strength. Since the temperature for both these samples are very close, it is easy to see the variation in this type of test.

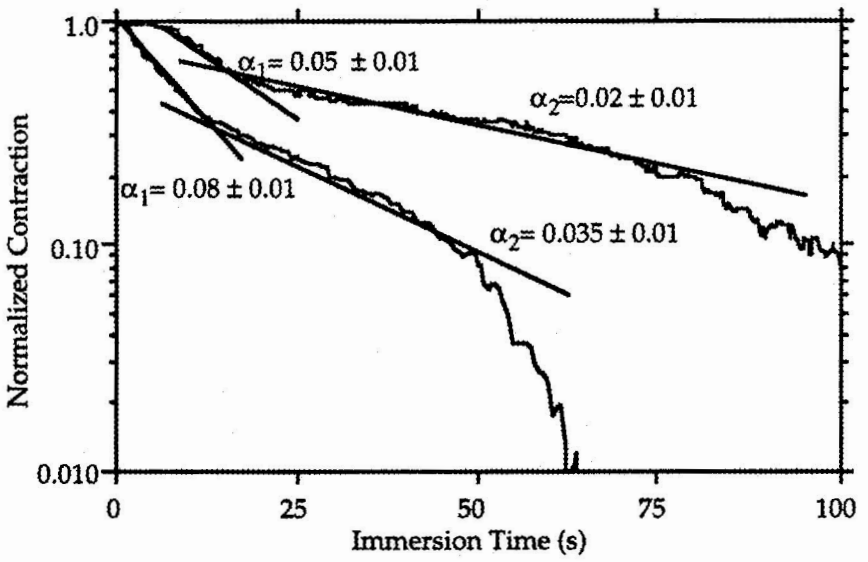

Figure 3.7: Plot of normalized position versus time on a semilog scale for two aorta samples in a heated waterbath at 71°C (α_1 and α_2 top line) and 89°C (α_1 and α_2 bottom line) pulled to 10% of yield strength.

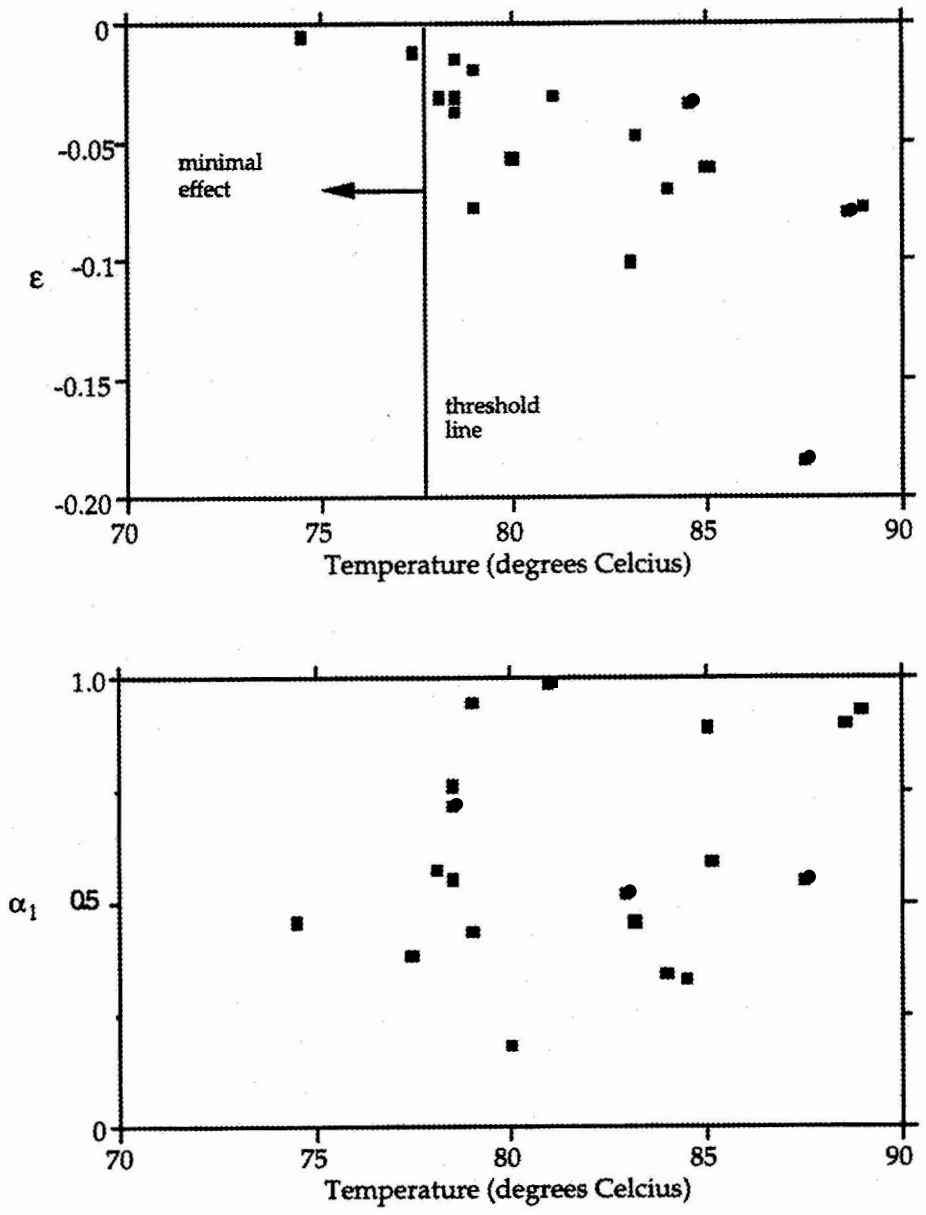

Figure 3.8: ϵ and contraction coefficient α_1 versus temperature for the 19 intestine samples tested. Two separate groupings appear in the ϵ plot, leading to a possible threshold effect at 77°C. The contraction coefficient is constant with temperature.

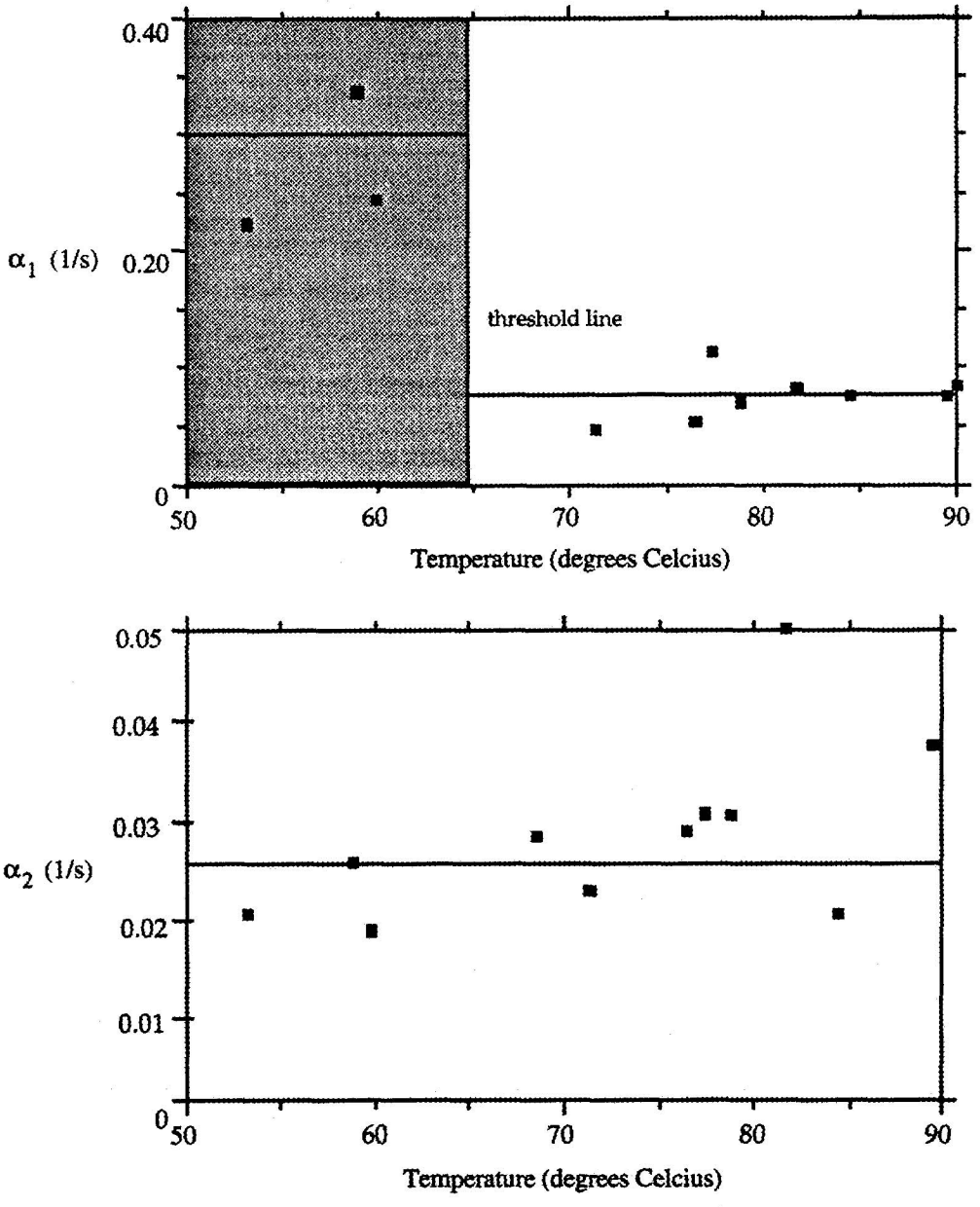

Figure 3.9: First and second coefficient of contraction versus temperature for aorta. The first coefficient, α_1, has a threshold trend with the threshold temperature at 65°C with an average of 0.3 ± 0.1 (1/s) below, and 0.07 ± 0.03 (1/s) above. The second has an average of 0.025 ± 0.02 (1/s) for the entire temperature range.

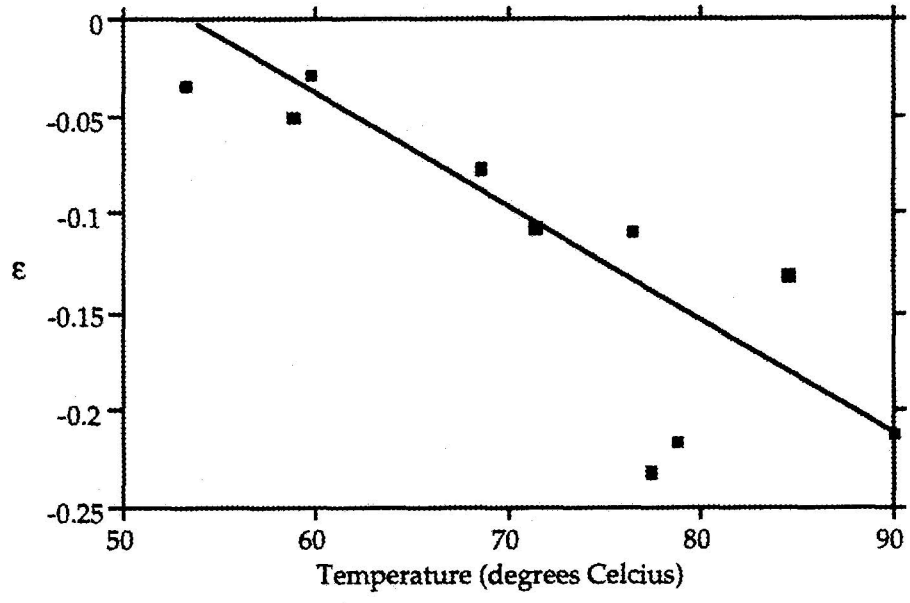

Figure 3.10: ϵ versus temperature for aorta samples. Strain for aorta has a linear relationship with temperature at a slope of -0.04 $\pm$ 0.004 (1/°C).

to its original shape after exposure, but rather appeared stretched out and thinner. However, no physical changes seemed to occur to the material itself; i.e., no change in color or texture were observed during or after testing.

3.2.2 Laser Tests

Laser irradiation of stained aorta and intestine causes less contraction than the waterbath tests. Contraction can be detected at a radiant exposure of 75 mJ/mm^2. For slow pulsing at about 1 Hz, very slight contraction can be seen with each pulse, on the order of 100 μm. Figure 3.12 shows a contraction in stained intestine when exposed to 50 pulses at about 3–4 Hz. A total contraction on the order of 2–3 mm starts after the 10th pulse, and continues until the end of pulsing. The tissue then starts to recover somewhat during the remainder of the test. Similar results are obtained with aorta with the largest contraction occurring at 50 pulses at 3–4 Hz. However, the amount of contraction was only 1 mm. No tests were performed for the elastin biomaterial because it does not stain well with ICG, and therefore would not absorb the laser light. Table 3.2 gives various contraction amounts for both intestine and aorta.

Table 3.2: Contraction amounts and their corresponding laser parameters for aorta and intestine samples cut with the die mold and stained with 6.5 mM ICG for 5 minutes. Pulse duration was 5 ms.

Tissue	Contraction (mm)	Number of Pulses	Pulse Interval (s)	Irradiation mJ/mm^2
intestine	0.2	30	1.0	30
	0.5	20	0.5	30
	2.0	50	0.5	75
aorta	400	50	0.5	30
	0.6	50	0.3	30
	1.0	30	0.3	75

Transmission at 808 nm measured during these tests generally started low (10%) and increased rapidly to 80–90% as the ICG stained layer bleached from green to orange.

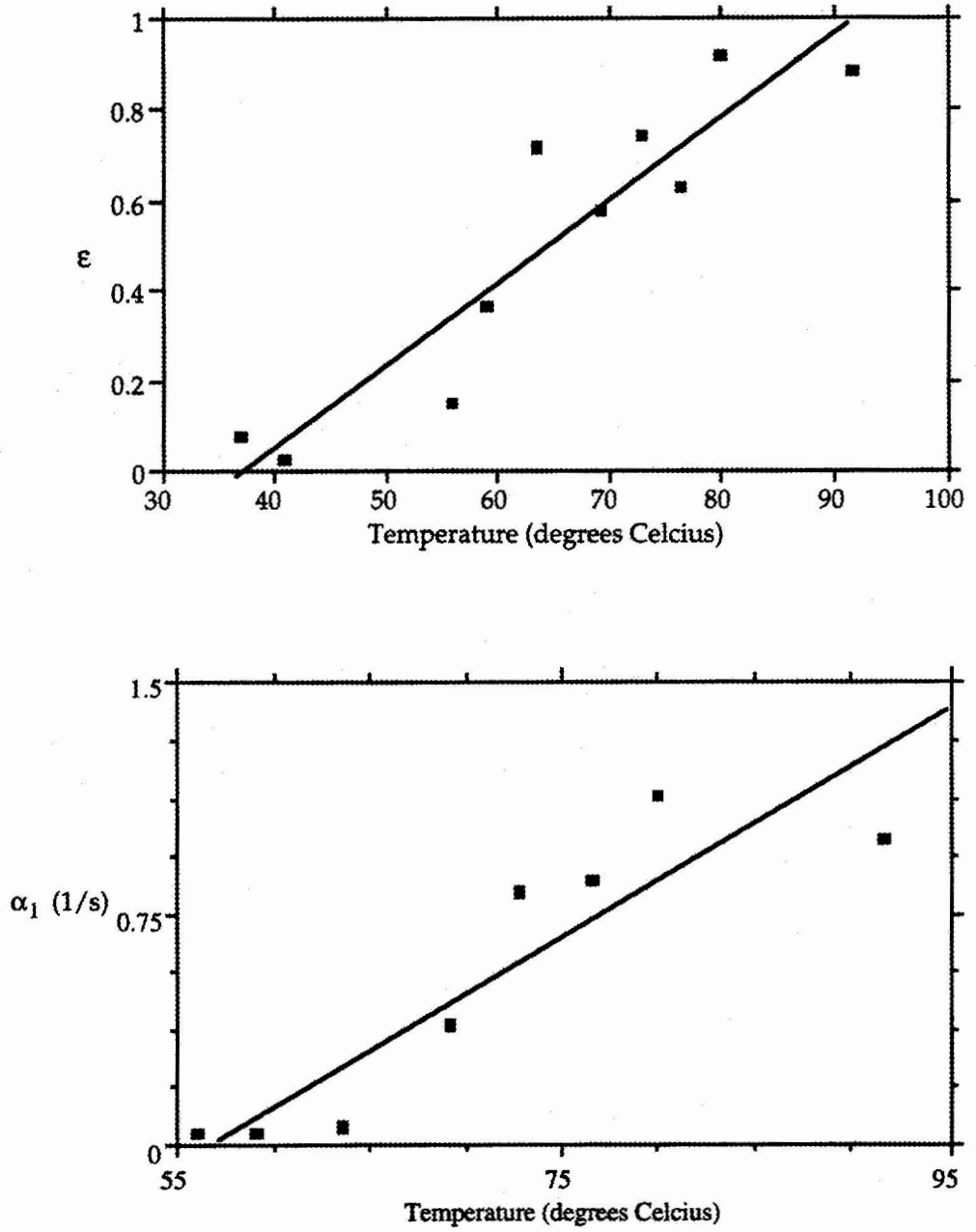

Figure 3.11: Plots of ϵ and α_1 for elastin biomaterial. The strain increases linearly with temperature at a slope of 0.015 ± 0.005 (1/°C), as does the coefficient of contraction α_1 with a slope of 0.036 ± 0.006 (1/s°C).

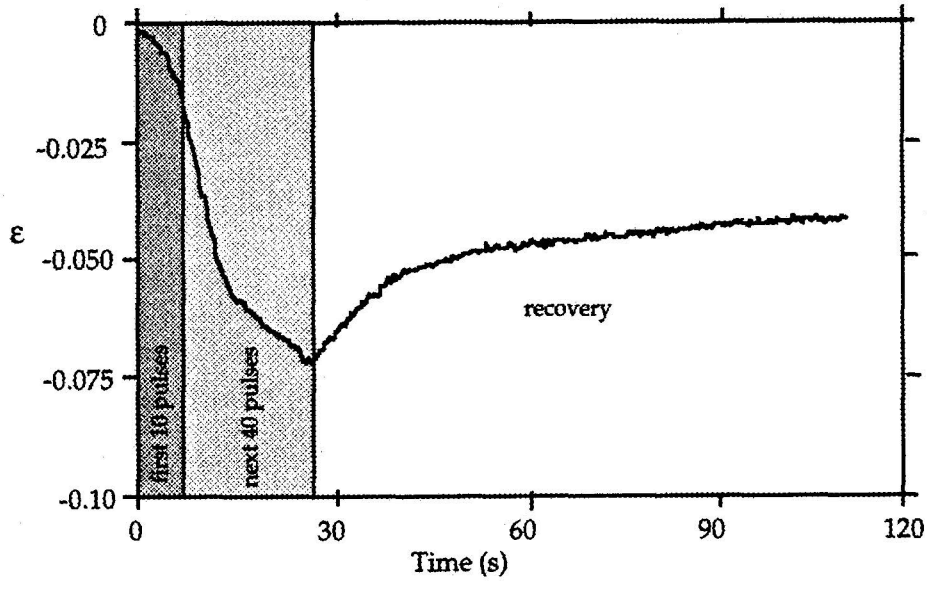

Figure 3.12: Contraction for stained intestine exposed to repetitive laser pulses at 3–4 Hz. Contraction starts after about 10 pulses, and continues until pulsing is stopped (50 pulses). The subsequent rebound in strain corresponds to the recovery of the tissue.

This transmission trend was the same for both intestine and aorta throughout all the laser tests.

3.3 Waterbath Tissue Welding

Waterbath welds were successful for all five tissue welds attempted: intestine to intestine, aorta to aorta, heterograft to heterograft, intestine to heterograft, and aorta to heterograft. Welds were possible for temperatures from 60–80°C and times 3–15 minutes. All intestine type welds exhibited a peak strength trend in both time and temperature, with peaks in strength between 70–75°C and 7–10 minutes. The welds containing aorta and/or heterograft exhibit a peak strength trend in temperature, but always increase in strength as time increases, up to 15 minutes (see Figures 3.13 and 3.14).

Table 3.3 gives the strongest waterbath weld obtained for each type, and the corresponding time and temperature.

Table 3.3: Strongest waterbath welds and their corresponding times and temperatures.

Weld type	Strength (N)	Time (min)	Temperature (°C)
intestine-intestine	2.3	10	65
aorta-aorta	2.8	15	70
heterograft-heterograft	1.5	15	70
intestine-heterograft	0.8	10	75
aorta-heterograft	0.4	15	75

3.4 Laser Welds

Laser welds of the intimal side of aorta to the intimal side of aorta were not successful. The transmission of unstained aorta was 85–90% and stained aorta was 10–20%, therefore most of the light is absorbed by the stained layer. It appears the intimal sides of aorta will not bond to each other at the short times required for laser welding. As many as 30 pulses at 75 mJ/mm^2 were fired at the sample, resulting in definite heating of the tissue,

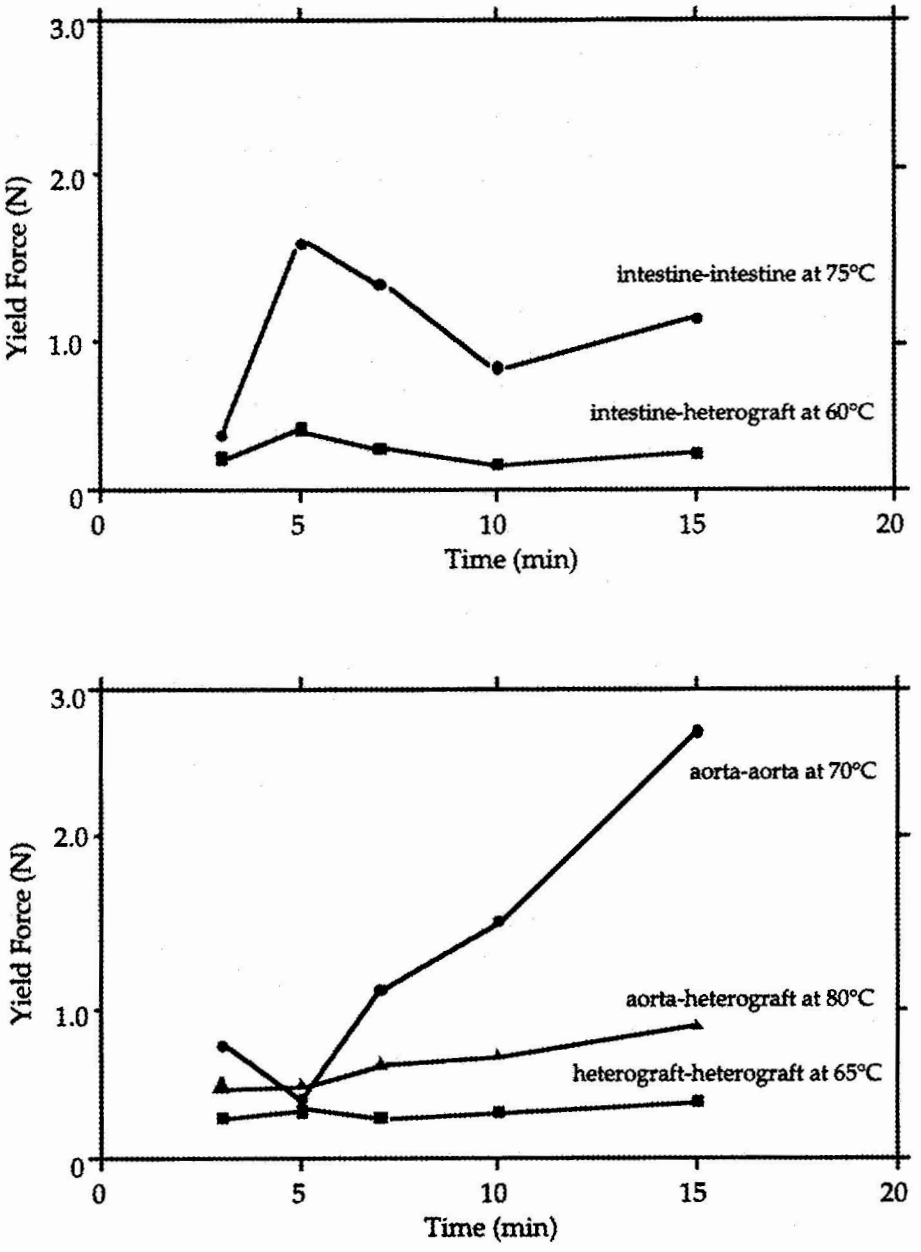

Figure 3.13: Yield force of various waterbath welds versus time in minutes.

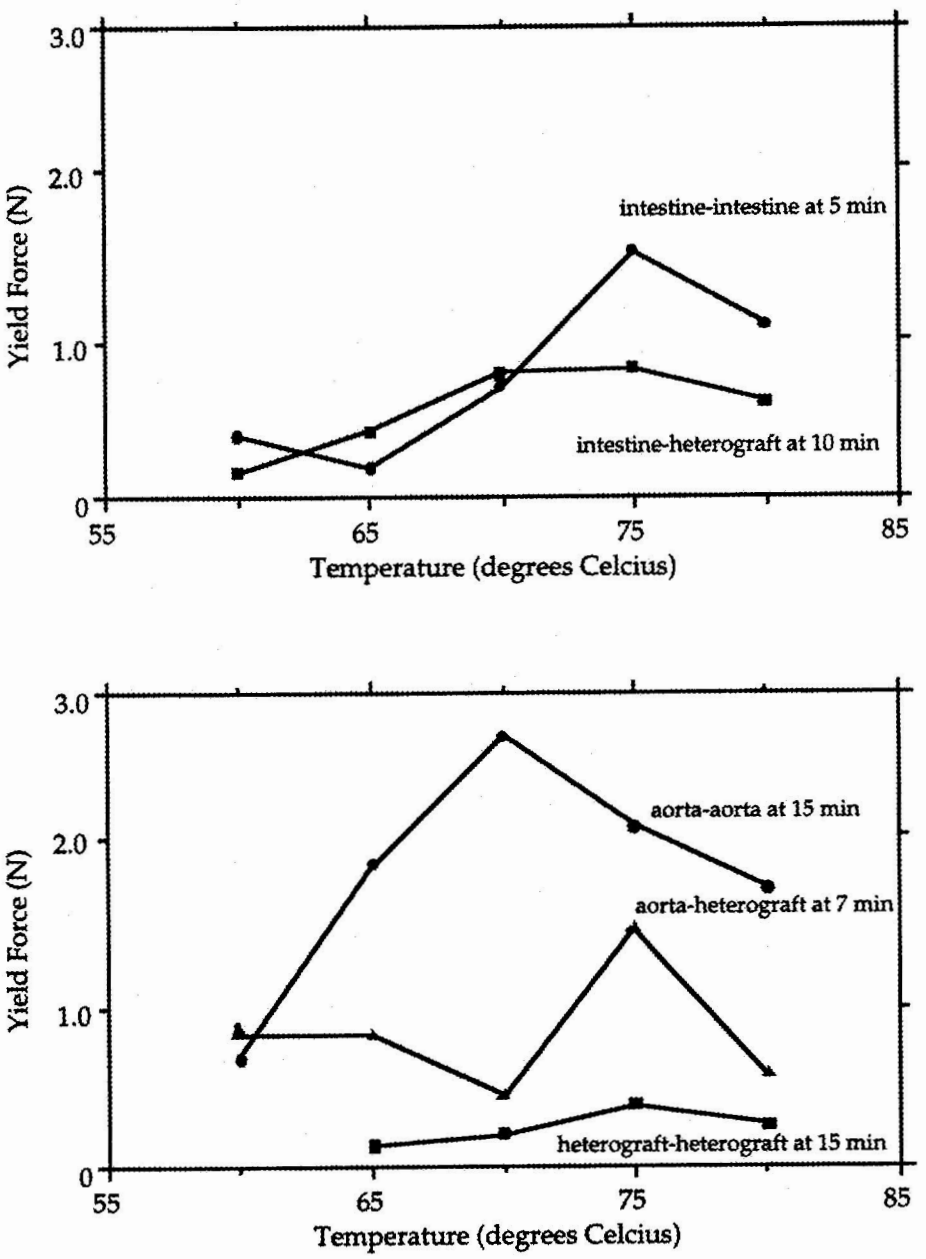

Figure 3.14: Yield force of various waterbath welds versus temperature in °C.

but no welding or bleaching of the stained layer. Table 3.4 gives the strongest laser welds produced in this study for the other four types.

Table 3.4: Strongest laser welds and their corresponding laser and staining parameters.

Weld type	Strength (N)	Irradiance (mJ/mm^2)	Stain Conc. (mM)	Number of Pulses
intestine-intestine	0.65	42	6.5	20
heterograft-heterograft	0.83	42	1.6	7
intestine-heterograft	0.81	42	1.6	20
aorta-heterograft	0.61	42	1.6	25

The strongest welds occurred at $42\,mJ/mm^2$ as well as a staining concentration of 1.6 mM, and more than 10 pulses. In these cases, parts of the stained layer remained fused to the unstained layer after the weld was pulled apart. Rarely was any bleaching of the stained layer noted at this irradiation. Figure 3.15 shows laser weld strengths compared to number of pulses. Trends in these graphs are similar to the waterbath welding studies.

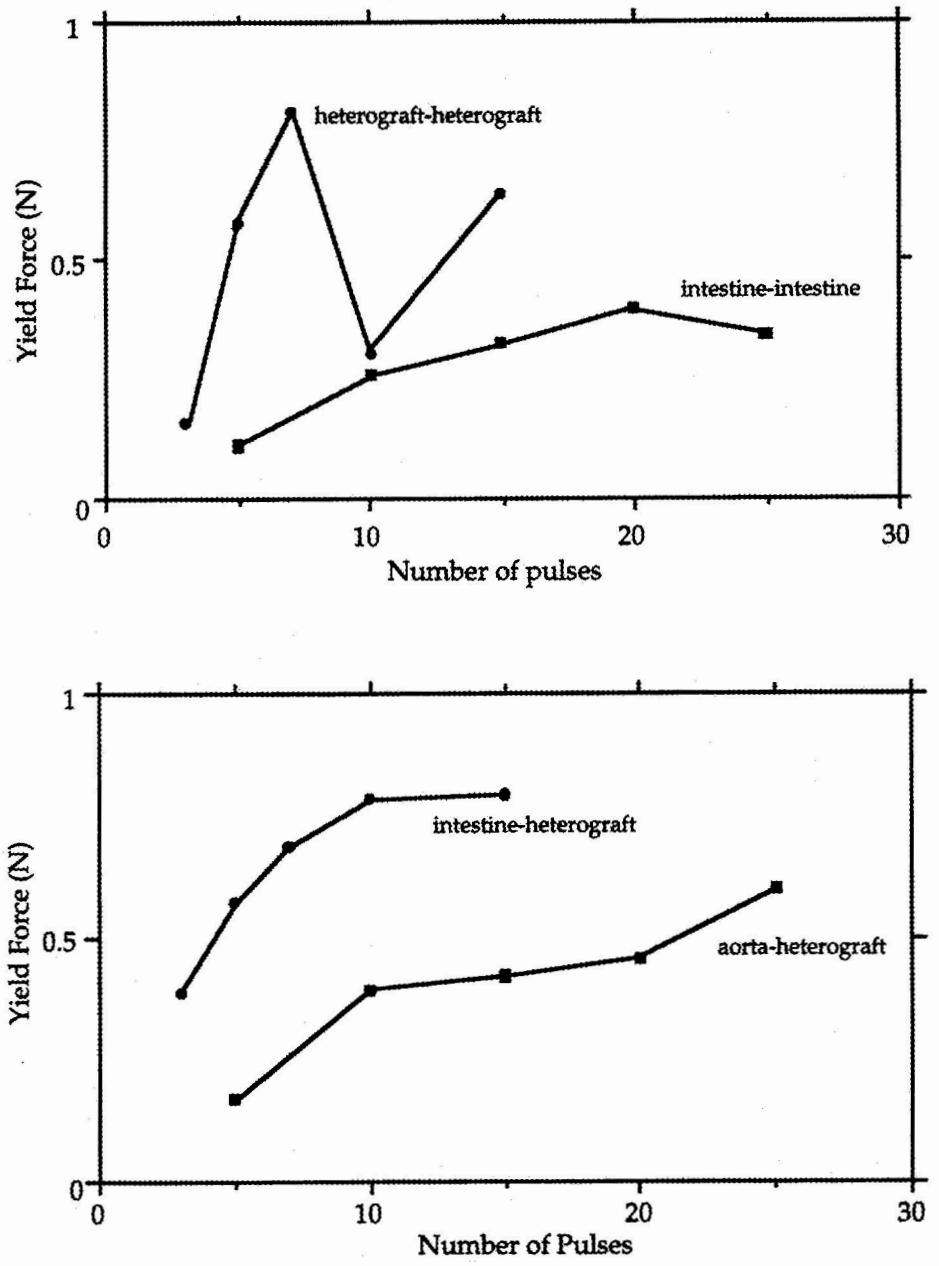

Figure 3.15: Intestine-intestine, heterograft-heterograft, and aorta-heterograft laser weld strengths at 1.6 mM staining concentration and 42 mJ/mm^2 irradiation, and intestine-heterograft laser weld strengths at 6.5 mM staining concentration and 70 mJ/mm^2 irradiation, for various pulse numbers.

Chapter 4

Discussion

The goals of this research included four methods in which to study the effects of heat and laser light on tissue: Yield strength comparisons, thermal contraction experiments, waterbath welding studies, and laser welding studies. All four of these studies are important to laser tissue welding because it is a thermal process even though the mechanism is not well understood. Studies of tissue characteristics are difficult due to tissue structure variability not only from sample to sample, but within one sample itself.

4.1 Yield Strength Tests

The 20–30% variation in tensile strength in each set of tissue samples is primarily due to differences in tissue thickness (see Table 3.1). The thickness varies from sample to sample and is difficult to measure accurately. Other factors of importance to overall strength include inconsistencies in the tissue, i.e., weak spots due to thin areas, and the size of the sample. Though all samples were cut with the die mold, there was still a 5–10% variability in size.

The tissue constituents collagen, elastin, and ground substance also vary, and contribute differently to tissue strength. Collagen and elastin act as the main strength components, accounting for the tissue's flexibility and elasticity. Similar results were found by Harkness *et al.* and Minns *et al.* where small differences in the microstructure of the tissue and differences in constituent content led to large variations in mechanical strength. Removal of collagen leads to a 80% decrease in stress at 20% strain. Ground

substance plays an important role in holding the collagen and elastin matrix together, and if it is removed, there is a 50% decrease in stress at 20% strain [16, 17]. Thus if each section of tissue has varied amounts of all three components, its strength will vary greatly.

4.1.1 Heated Yield Strength Tests

Heating tissue causes structural changes due to denaturation of collagen and other proteins. This results in tissue contraction and coagulation. These structural changes have minimal effect on the overall tensile strength of the tissue. The average strength for preheated intestine and aorta were within 10% of their unheated average strengths. Harkness *et al.* reported that removing certain constituents would be the main cause for any weakening of tissue [17]. Since heat causes a change in structure, but does not remove any tissue components, no significant change in strength can be seen in these tests.

4.1.2 Laser Yield Strength Tests

Laser irradiated tissue shows changes in structure as the heat produced in the absorbing layer diffuses through the entire sample thickness. This changes are evidenced by the changes in color, texture, and size of the sample. Roider*et al.* reported that repetitive exposure of short (5 μs) laser pulses resulted in microphotocoagulation, or selective damage to certain absorbing structures [29]. Although heating in a waterbath did not change the mechanical strength, all temperatures were below 100°C, the point where charring can occur. Repetitive laser pulsing results in temperatures greater than 100°C, causing desiccation, and charring of part of the tissue surface, resulting in a decrease in mechanical strength (Figure 3.2). This is evidenced by the observation of charred spots on the tissue surface after irradiation. Exposing the tissue to 15–25 pulses results in a 20–25% decrease in average tensile strength.

Yield strength tests in all three cases (untreated, waterbath heat, laser heat) are similar given the large variations due to structure and thickness that occur in all the tests.

Heating the entire tissue sample in a waterbath did not markedly decrease strength. In contrast, the samples exposed to laser irradiation gave average strengths 20–25% less than the untreated and waterbath samples. However, the standard deviation associated with the untreated samples is 25% for intestine, and 40% for aorta. Since the decrease in strength associated with laser irradiation is within this deviation, laser irradiation does not decrease the overall average strength of the tissue enough to be a strong concern during laser welding.

4.2 Thermal Characterization

4.2.1 Waterbath Tests

The changes observed in each tissue sample are typical of most biological samples exposed to heat. Protein denaturation and coagulation caused changes in color, texture, and size. The rates at which these changes occur can be of importance to laser welding.

The contraction of porcine intestine upon heating is due to the high concentration of type I collagen in the smooth muscle cell layers (see Table 4.1). Contraction occurred at a rate of $0.6 \pm 0.1\ s^{-1}$. Originally, I thought intestine would have the same damage characteristic based on the Arrhenius model as Agah *et al.* reported for aorta [8]. However, when the same numerical method is used, the plot of temperature versus α_1 produced has no linear trend (see Figure 3.8).

The strain-temperature relationship for intestine showed two unique rate groupings, indicating a threshold mechanism for contraction. A three-fold increase in the amount of strain was observed above 77 ± 1°C (see Figure 3.8). Thus, even though contraction occurs at a constant rate (within variation) for increasing temperature, strain increases dramatically above the threshold temperature. The average strain below threshold is -0.01 ± 0.004, while the average above threshold is -0.05 ± 0.04. The variation in the contraction rate is most likely due to collagen variations from sample to sample (about 25% [17]). This threshold characteristic could be unique to intestine, or more specifically, to high concentrations (above 50%) of Type I collagen in the tissue structure. Because

of the threshold mechanism, laser welds could be consistently strong under a variety of parameters, as long as the threshold temperature is reached.

Porcine aorta exhibited two different contraction characteristics having two different trends in temperature (see Figure 3.9). The first coefficient was calculated from the first 5–10 seconds of heat exposure (see Figure 3.7). This coefficient has the same threshold trend as seen with intestine, with a threshold temperature of 65 ± 5°C, where the rate of contraction above threshold is $0.07 \pm 0.03\,s^{-1}$. The second coefficient may slightly increase with increasing temperature, but is primarily characterized by a constant rate of contraction of $0.025 \pm 0.02\ s^{-1}$. The two different contraction rates may be due to more than one type of collagen present, which denature at different temperatures [14]. Types III and V collagen are relatively hydroxyproline rich, which stabilizes the helical formation of collagen molecules, resulting in greater temperature stability [30].

The strain-temperature relationship for aorta is also linear with a slope of -0.04 ± 0.004 (1/°C) (see Figure 3.10). The increase in total strain (total contraction) corresponds with the increase in contraction rate with temperature.

Table 4.1 gives the contraction rate α_n and average collagen content for intestine and aorta. Intestine collagen contents were approximated by comparison of the contraction rates since I was unable to find a source for average collagen content in intestine. Given that intestine has a much higher contraction rate, its average collagen content will be much higher than that of aorta.

Table 4.1: The average tissue contraction coefficients α_1 and α_2 for intestine and aorta and collagen content. Intestine content is approximated from contraction rate comparison, and from reported collagen content of aorta by Harkness.

Tissue	contraction rate (1/s)	average collagen content (%)
intestine (α_1)	0.6 ± 0.1	75 ± 20
aorta (α_1)	0.07 ± 0.03	50 ± 25
aorta (α_2)	0.025 ± 0.02	50 ± 25

The strong variation in contraction can also be correlated with the amount of collagen in a particular section of the tissue. Collagen denaturation is the main cause of contraction, and its content is dependent upon where the section is from: i.e., for intestine, whether it is from the small or large intestine or from the colon; and for aorta, how close it is to the heart. Collagen content is inversely proportional to tissue stretch, therefore higher content allows the sample to stretch less under the same amount of force.

Similar contraction characteristics were observed by Solhpour *et al.* on bovine tendon. Gross spontaneous shrinkage occurred between 74 and 81°C. Optical birefringence of the collagen fibrils, strong in normal collagen, was lost at these temperatures—leading to probable denaturation and coagulation of the collagen structure. However, no trends of contraction or strain were reported [31].

Variation in mechanical and thermal characteristics are due to microstructure variations within the different tissues [14, 16, 17]. If the collagen fibrils are intertwined in different manners within a segment of tissue, then both its thermal and mechanical characteristics will vary. Because of these inconsistencies, exact determination of thermal parameters is difficult, and not without strong variations of 20–30% or more. These sources indicate that most thermal and mechanical parameters differ for each tissue type, and even with accurate testing, many variations will exist.

Lengthening of the biomaterial with increasing temperature is most likely due to the lack of any contracting constituent, as well as destroyed bonds within its microstructure. Applying a constant force to the material causes the molecular structure to strain, and if some of the molecular bonds holding the tissue together are broken by the heat, the biomaterial will increase in length as the force is held constant. This lengthening is most likely due to the breakdown of fibrin at the temperatures used, therefore destroying the bonds which hold the biomaterial together.

4.2.2 Arrhenius Rate Analysis

One approach for modeling thermal damage for aorta and intestine is based on an Arrhenius damage model first proposed by Henriques to determine the kinetic process of

thermal damage to tissue [8,32]. This model is typical of physical and chemical processes and can be described by the following equation:

$$\Omega(t) = -\ln\left(\frac{n(t)}{n(0)}\right) = A\int_0^t \exp\left(-\frac{\Delta E}{RT}\right) dt \tag{4.1}$$

where

$\Omega(t)$	=	accumulated damage (unitless)
$n(0)$	=	number of native molecule originally present (unitless)
$n(t)$	=	number of native molecule at time t (unitless)
A	=	frequency factor (s^{-1})
ΔE	=	activation energy (J/mol)
T	=	temperature (K)
t	=	heating time (s)

Agah *et al.* [8] determined the kinetic coefficients A and ΔE by defining $\Omega(t) = 1$ as "just noticeable damage." Since Agah *et al.* held the temperature constant for a specified period of time, the Arrhenius model reduces to:

$$\ln(t) = -\ln(A) + \frac{\Delta E}{R}\frac{1}{T} \tag{4.2}$$

Thus a plot of $1/T$ versus $\ln(t)$ would be linear, with a slope of $\Delta E/R$ and an intercept equal to $-\ln(A)$, therefore providing experimental estimates of A and ΔE.

The process of contraction or expansion appeared to be an exponential change in position with respect to time. The rate at which this change occurred is related to temperature, as well as the properties A and ΔE for each tissue. Thermodynamically, the frequency factor A is related to ΔS, or change in entropy of reaction, and ΔE is equal to ΔH, or change in enthalpy of reaction. These two quantities define a first-order reaction rate process, which is the theoretical model for thermal tissue damage. Plots of $1/\alpha_n$ versus inverse temperature can give values to the thermal damage parameters A

and ΔE. However, a plot of $1/\alpha_1$ versus inverse temperature for intestine has no linear trend, and a plot of $1/\alpha_2$ versus inverse temperature has only a very slight linear trend (see Figure 4.1). If a slight linear slope is used, the values for A and ΔE calculated from a plot of $1/\alpha_2$ and $1/T$ in (K) for porcine aorta are as follows:

$$A = 2.49 \times 10^{73} \qquad (\text{range} = 10^{45} - 10^{101})^*$$
$$\Delta E = 600 \pm 185\,\text{kJ/mol}$$

These values for A and ΔE are comparable to Agah's findings for human aorta ($A = 6 \times 10^{63}$, $\Delta E = 430 \pm 85\,\text{kJ/mol}$). Their values have a 20% variation, while I have a 30% variation, which I feel is reasonable given the large differences among tissue samples. Also, differences in human and porcine aorta may account for the discrepancy between the two study results. However, since the rate for intestine was constant, and the rate for aorta had only a slightly increasing linear slope, I feel this is not a very useful model to represent thermal changes in tissue with respect to increasing temperature.

4.2.3 Laser Tests

Laser exposure of the tissue caused bleaching of the stained layer, as well as desiccation and charring of the tissue for high numbers of repetitive pulses (above 10 pulses). The amount of contraction observed was smaller (5–50%) when compared to the waterbath tests, depending on how many pulses were fired. This is mainly due to a reduced area of heating of about 10–20% of the area heated in the waterbath. Contraction typically started after about 10 pulses at energies above $75\,\text{mJ/mm}^2$, and was only a few hundred microns. The maximum contraction was about 2 mm after 50 pulses (see Table 3.2). Because thermal contraction requires at least 10 pulses, strong welds mediated by this thermal change will need multiple pulses.

The waterbath tests produced greater contraction than the laser tests without the side effects of desiccation or charring. Intestine contracted the most in both the waterbath

*It is easier to report a range of values here instead of a standard variation, since this number is incredibly large.

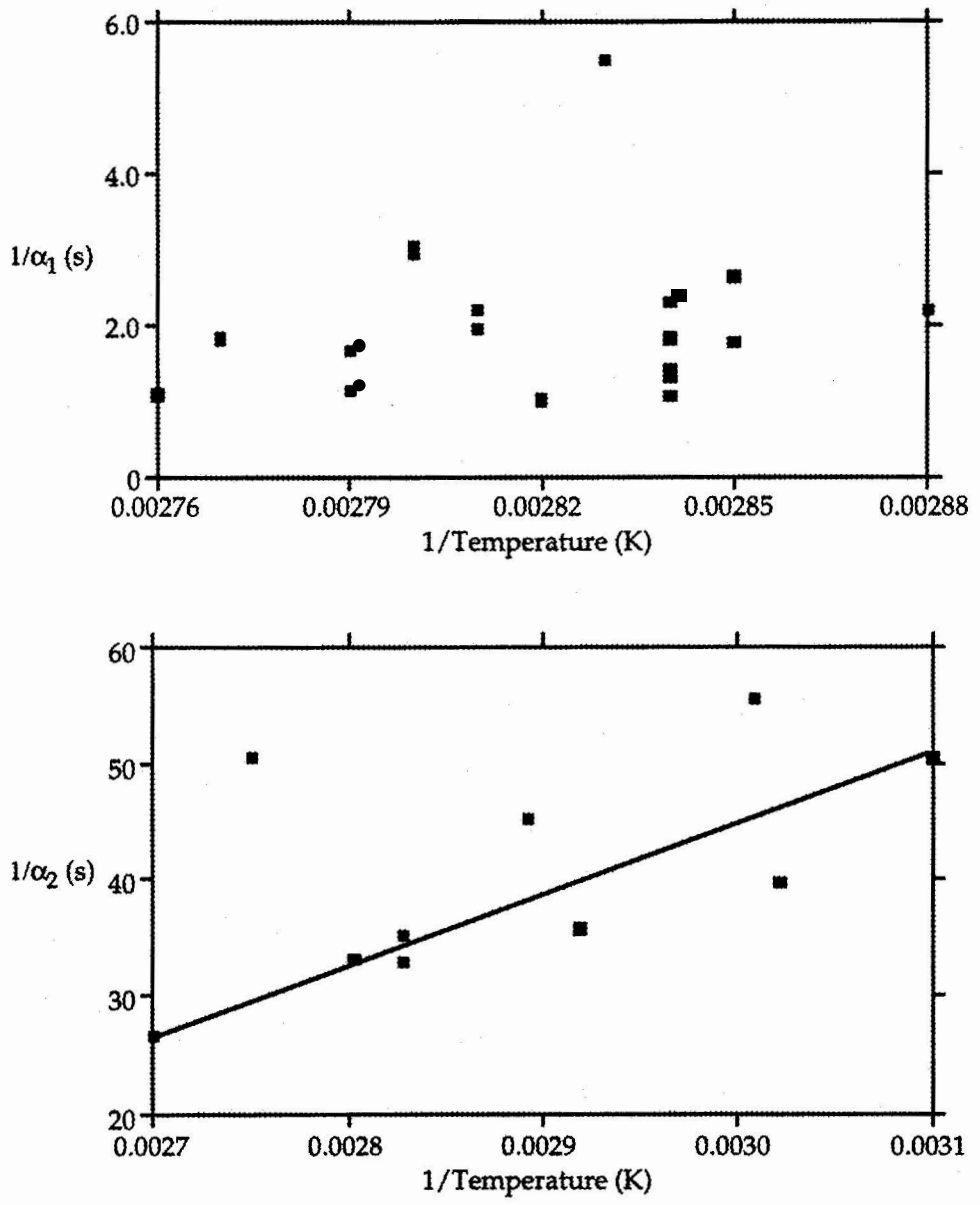

Figure 4.1: $1/\alpha_1$ and $1/\alpha_2$ versus inverse temperature (K) for intestine and aorta, respectively. The intestine plot shows no linear trend, while the aorta plot shows a linearly increasing trend.

and laser tests, which correlates with increased collagen content. The waterbath samples also caused more dramatic changes in color, size and texture when compared to the laser samples. Since the laser contraction rates were small, and the heating not as uniform as the waterbath, I did not determine any rates of contraction, or strain-temperature relationships.

4.3 Waterbath Tissue Welding

Welding tissues using a constant temperature waterbath is a good way to accurately determine the proper temperature and time to obtain the optimum weld strength upon cooling of the tissues. Welds were strongest at lower temperatures for longer periods of time. Since the strongest welds were all produced at times above 10 minutes, the welding mechanism in a waterbath is rather slow. Similar results were reported by Solhpour *et al.* where waterbath welding of bovine tendon (primarily type I collagen) was optimal at temperatures between 58 and 62°C and a time of 20 minutes. Optical birefringence of the fibrils exists in this temperature range, and a small area of decreased birefringence can be seen right along the weld line [31]. Given the time suggested for optimum welding of tendon, it is possible that welding of aorta would be strongest at times greater than the maximum 15 minutes used in these waterbath experiments. The strongest waterbath welds for intestine are at 10 minutes with a temperature between 65 and 75°C, right below the transition temperature for contraction of the collagen fibrils in the smooth muscle walls.

4.4 Laser Tissue Welding

Failure to laser weld the intimal surfaces of porcine aorta together has been reported in previous studies [28]. Porcine aorta was quite thick (2–3 mm) and may not create a confined welding spot because of tissue scattering and spreading of the irradiated area. This can be seen in the overall heating of the two tissue layers, but not enough localized heating to create a weld at the stained layer depth. Also, there may be a lack of unbound

collagen at the intimal surface, which is needed in order to produce a bond. The pressure used in the laser welding studies may have not been enough to create any weld of this type. Lastly, the heating time may be too short, as seen in the long waterbath welding times.

The remaining four types of laser welds have notable characteristics, especially when an optimal weld is produced. Temperatures can be estimated using the following equation:

$$\Delta T = \frac{\mu_a E}{\rho c} \tag{4.3}$$

Here, ΔT is change in temperature, ρc is the heat capacity (approximated as the value for water, $4.2\,\mathrm{J/cm^3}$), E is laser irradiation in $\mathrm{mJ/mm^2}$, and μ_a is the absorption coefficient. A transmission measurement gives μ_a by the following equation:

$$\mathcal{T}_s = \mathcal{T}_u exp(-\mu_a d) \tag{4.4}$$

Where $\mathcal{T}_s$ is stained transmission, $\mathcal{T}_u$ is unstained transmission, and d is the depth of the stained layer. Using a transmission of 20% for stained tissue [†] and a depth of 25–75 μm [‡], the absorption coefficient can be approximated as $215–640\,\mathrm{cm^{-1}}$. Thus at $42\,\mathrm{mJ/mm^2}$, ΔT is 22–64°C, giving tissue temperatures of 57–89°C. This wide temperature estimation is due to the variation in accurate staining depth measurements (see section 1.2.3). Also, higher irradiations would easily bring the temperature at the weld site above 100°C, resulting in charring of the stained layer.

Lower energies produced the strongest weld in all four cases, and lighter staining in three of the four cases (see Table 3.4). For these welds, rarely was any bleaching noted at the weld site, and usually only at the edges where the stained layer had direct laser exposure. The lower staining concentration produced better welds because it may be more uniform than the 6.5 mM concentration. 6.5 mM is the saturation point for ICG in water, and therefore some ICG is usually not completely dissolved in the water, leading to

[†] Transmission was measured on aorta samples exposed to $21\,\mathrm{mJ/mm^2}$, with a 1.6 mM stain for 5 minutes.

[‡] measured via flubrescence microscopy.

a "graininess" in the tissue stain. This graininess creates less uniformity in the stain, and increases the likelihood of hot spots when irradiated. These hot spots are evidenced by small charred areas at the weld site when the highest staining concentration is used with the highest irradiation. Lower ICG concentrations provide less absorption, and therefore lower peak temperatures during the laser pulse. Thus, enough heat is produced to create a weld without causing a lot of collateral thermal damage such as charring. Photothermal bleaching of the ICG layer was rarely seen at $42\,mJ/mm^2$ irradiance, but usually seen $70\,mJ/mm^2$ irradiance, resulting in weaker welds for all four types. Therefore, bleaching is not necessarily a sign of welding, but rather a possible sign of excessive heating. $70\,mJ/mm^2$ produced bleaching and dessication to the stained layer, and even charring at high pulse numbers.

4.5 Waterbath versus Laser Welding

Waterbath and laser welding are two different ways to obtain a bond between two tissue surfaces. However, is the actual mechanism for waterbath welding the same as the mechanism for laser welding? This is rather difficult to answer. Past studies link collagen to the welding process [9, 19], where individual fibers unwind at temperatures above denaturation, and rebind with collagen fibers from the apposed tissue surface [14]. If this is the only source of a welding bond, then the huge discrepency in welding times between waterbath (5–15 minutes) and laser (5–15 seconds) is somewhat of a mystery. Laser welding quickly heats an extremely confined area of the stained layer, whereas the waterbath slowly heats the entire tissue. Confining the heat to a small area reduces the welding time dramatically, as reflected in the times above. This leads to another problem: what time is really needed for the process of collagen binding to occur? The large time differences could indicate that there are two different mechanisms for welding in waterbath and via the laser. Also, the ability to weld heterografts to each other in both waterbath and laser welding studies leads to other welding constituents, since heterografts contain very little collagen.

Similar trends exist the laser weld studies as in the waterbath weld studies. Intestine to intestine exibited a peak strength before the highest number of pulses for both staining concentrations and laser irradiances. Heterograft to heterograft and intestine to heterograft had the same peak strength trend for 1.6mM ICG concentrations at both irradiances, but increasing strength for the higher ICG concentration. Aorta to heterograft welds had increasing strengths for both irradiances and stains, at least for the number of pulses used. Peak strength may not have been reached with the highest number of pulses used in each experiment set. These trends show that longer times are needed to produce stronger welds under both conditions: waterbath and laser.

Possibly, collagen denaturation and rebinding is a process that starts very quickly, but is slow to build a matrix of bonds to connect the two tissue surfaces. Thus the mechanism started in the laser welds has adequate time to build the matrix of bonds in the waterbath welds. This would explain the reasons why welds are possible with laser irradiation, but are typically 30–50% as strong as the waterbath welds. Another observation to support this idea is the ability to obtain weaker welds at lower temperatures and less time in the waterbath, or fewer pulses with the laser. Another possible reason for weaker laser welds is less pressure applied to the weld site. The pressure of the binding clip is much greater than the 2 kg weight used in the laser studies. Weld surface area should not be a factor, since the tissues were overlapped in the same fashion for both studies. Overall, laser welding produced less damage to the surrounding tissue since only the weld site was heated, rather than the entire tissue volume. This is seen in the contraction and change in color of both tissues in the waterbath welds. Since one purpose of welding is to create a bond with little or no collateral thermal damage, perhaps one would accept the decreased welding strength in return for less damage to the tissues.

4.6 Summary

Several different conclusions can be drawn from the tests in each study. In the yield strength studies, I found measurement of yield strength varied due to tissue structure

and thickness. Additionally, heating of the tissue samples via a steady-state waterbath had no effect on yield strength, while repetitive laser pulsing caused a 20–25% decrease in yield strength. This in important when considering the possible ramifications of repetitive laser pulsing on the strength of the tissue itself, not just the strength of the weld created.

The waterbath and laser thermal characterization led to several conclusions. First, I discovered two different thermal mechanisms, one occuring in intestine, and both occuring in aorta. Ths first is a threshold mechanism where contraction occurs at 0.6 $\pm$ 0.1 s^{-1} above 77°C for intestine, and at 0.07 $\pm$ 0.03 s^{-1} above 65°C for aorta. The second may be a linear damage mechanism following the Arrhenius model, resulting in calculations of A, the frequency factor, and ΔE, the activation energy. These findings lead to possibly more than one mechanism involved in the welding process, as well as different mechanisms for different tissue types. Also, some tissues (i.e. aorta) may have more than one mechanism, as reflected by the two different contraction rates. The laser contraction tests demonstrated that contraction occurs during laser irradiation as well as in a waterbath. This shows that similar temperatures are reached in both cases, and contraction is a problem associated with the laser welding process. The fact that two elastin heterografts could be welded together in both waterbath and via laser gives rise to other welding mechanisms, since they contain very little if no collagen at all. Lastly, the decrease in strength in the biomaterial with heat exposure leads to problems in biomaterial-tissue welding. If the biomaterial weakens upon exposure to heat when welded to tissue, a poor weld will be produced. This study shows much work is needed to improve biomaterial strength and durability before it can be readily used in laser welding.

Waterbath tissue welding was of importance because it helped pinpoint the temperatures and times needed for an optimal weld. Waterbath welding also produced the strongest set of welds for each tissue type, which served as a basis for optimal welding strengths. These tests further support the idea of different mechanisms for each different tissue, as reflected by peak welding temperatures and times. The peak temperatures

were higher for intestine, and the peak times were longer for aorta and heterograft. The results of these studies reinforced Solhpour's findings of narrow temperatures and times for optimal welding in a waterbath. Lastly, welding via waterbath gave insight into the times and temperatures needed to produce a weld that is consistently strong.

Laser welding of all the tissue types suggests several conclusions. First, laser welding of aorta to aorta was impossible under the conditions used for all the other laser welds. Thus, welding of the intimal sides of aorta, which has been attempted in several other studies, may not be a viable option when attempting aortic wound closure. However, end-to-end welding, or anastomosis could still be used. Second, most all the optimal welds were created at a staining concentration of 1.6 mM, a laser irradiation of 42 mJ/mm^2, and more than 10 pulses. This connects laser welding to the laser contraction tests, where enough heat to start contraction was not created until after at least 10 pulses. Third, the estimated temperatures for these laser welds were between 57–89°C, which encompasses the range for threshold contraction from the waterbath characterization studies. Lastly, strong, reliable welds were produced at the above staining concentration and laser parameters, which provides a basis for future welding attempts with each type of tissue used.

The overall goal of this reasearch was to improve the reliablilty of laser welding through a thorough investigation of the mechanism of welding for each tissue type. The effect of heat and repetitive laser pulsing on mechanical strength was determined. Each tissue was characterized by extensive thermal studies to find the effects of temperature on welding components. Moreover, several welds were attempted in a waterbath and via laser irradiation to determine the best parameters for optimal welding. These parameters included time, temperature, staining concentration, laser energy, and pulse number.

Several more studies need to be done to determine the long term reliability of laser welds, as well as the long term effects laser welding has on the surrounding tissues. There are still several unknowns in the laser welding mechanism that need further examination. These include the discrepencies between waterbath and laser studies, the differencies in total laser exposure for optimal laser welds in each tissue type, and the interaction

between ICG, heat, and tissue. However, laser welding is possible and consistent under a variety of conditions, and therefore shows promise as a future alternative to sutured closure.

Bibliography

[1] S. D. DeCoste, W. Farinelli, T. Flotte, and R. R. Anderson, "Dye-enhanced laser welding for skin closure," *Lasers Surg. Med.*, vol. 12, pp. 25–32, 1992.

[2] V. L. Martinot, S. R. Mordon, V. A. Mitchell, P. N. Pellerin, and J. M. Brunetaud, "Determination of efficient parameters for argon laser-assisted anastomoses in rats: macroscopic, thermal and histological evaluation," *Lasers Surg. Med.*, vol. 15, pp. 168–175, 1994.

[3] M. C. Oz, H. W. Popp, M. R. Treat, L. S. Bass, and S. Popilskis, "*In vivo* comparison of THC:YAG laser welding to sutured closure of biliary tissue," *The Am. Surgeon*, pp. 275–279, May 1991.

[4] D. K. Dew, L. Supik, C. R. Darrow, and G. F. Price, "Tissue repair using lasers: a review," *Orthopedics*, vol. 16, pp. 581–587, 1993.

[5] S. L. Jacques, "Role of tissue optics and pulse duration on tissue effects during high-power laser irradiation," *Appl. Opt.*, vol. 32, pp. 2447–2454, 1993.

[6] W. de Gruytes, *Concise Encyclopedia of Biochemistry*. Berlin: New York, 1983.

[7] F. C. Henriques, "Studies of thermal injury. V. The predictability and the significance of thermally induced rate processes leading to irreversible epidermal injury," *Arch. Pathology*, pp. 489–501, 1946.

[8] R. Agah, J. A. Pearce, A. J. Welch, and M. Motamedi, "Rate process model for arterial tissue thermal damage: implications on vessel photocoagulation," *Lasers Surg. Med.*, vol. 15, pp. 176–184, 1994.

[9] J. A. Pearce and S. Thomsen, "Kinetic models of laser-tissue fusion processes," *Biomed. Sci. Inst.*, pp. 355–360, 1993.

[10] R. Marcuz, M. P. Riberio, J. M. G. Brum, C. A. Pasqualucci, J. Mnitentag, D. G. Bozinis, E. Marques, A. D. Jatene, L. V. Decourt, and E. Armelin, "Laser surgery in enclosed spaces: a review," *Lasers Surg. Med.*, vol. 5, pp. 199–218, 1985.

[11] J. T. Walsh, T. J. Flotte, and T. F. Deutsch, "Er:YAG laser ablation of tissue: effect of pulse duration and tissue type on thermal damage," *Lasers Surg. Med.*, vol. 9, pp. 314–326, 1989.

[12] W. Gorisch and K. P. Boergen, "Thermal collagen shrinkage promotes laser-induced vessel occlusion," in *Third International Congress in Laser Surgery, Austria*, pp. 26–29, 1979.

[13] R. D. Harkness, "Mechanical properties of collagenous tissues," in *Treatise on Collagen* (B. S. Gould, ed.), vol. 2, ch. 6, Academic Press, 1968.

[14] L. S. Bass, N. Moazami, J. Pocsidio, M. C. Oz, P. LoGerfo, and M. R. Treat, "Changes in Type I collagen following laser welding," *Lasers Surg. Med.*, vol. 12, pp. 500–505, 1992.

[15] W. Gorisch and K. Boergen, "Heat-induced contraction of blood vessels," *Lasers Surg. Med.*, vol. 2, pp. 1–13, 1982.

[16] R. J. Minns, P. D. Soden, and D. S. Jackson, "The role of the fibrous components and ground substance in the mechanical properties of biological tissues: a preliminary investigation," *J. Biomechanics*, vol. 6, pp. 153–165, 1973.

[17] M. L. R. Harkness and R. D. Harkness, "The use of mechanical tests in determining the structure of connective tissues," *Biorheology*, vol. 10, pp. 157–163, 1973.

[18] R. A. White, G. Kopchok, C. Donayre, R. Lyons, G. White, S. R. Klein, D. Pizzurro, R. P. Abergel, R. M. Dwyer, and J. Uitto, "Large vessel sealing with the argon laser," *Lasers Surg. Med.*, vol. 7, pp. 229–235, 1987.

[19] R. A. White, G. Kopchok, S. Peng, R. Fujitani, G. White, S. Klein, and J. Uitto, "Laser vascular welding—how does it work?," *Ann. Vasc. Surg.*, vol. 1, pp. 461–464, 1986.

[20] R. M. Fujitani, R. A. White, G. E. Kopchok, S. Peng, G. H. White, and S. R. Klein, "Biophysical mechanisms of argon laser-assisted vascular anastomoses," *Current Surg.*, vol. 45, pp. 119–123, 1988.

[21] A. Serure, E. H. Withers, S. Thomasen, and J. Morris, "Comparasion of carbon dioxide laser-assisted microvascular anastomoses and conventional sutured anastomosis," *Surg. Forum*, vol. 34, pp. 634–636, 1984.

[22] A. F. Badeau, C. E. Lee, J. R. Morris, S. Thompsen, E. G. Malk, and A. J. Welch, "Temperate response during microvascular anastomosis using milliwatt CO_2 laser," *Lasers Surg. Med.*, vol. 6, p. 179, 1986.

[23] M. Epstein and C. B. Cooley, "Electron microscopic study of laser dosimetry for microvascular tissue welding," *Lasers Surg. Med.*, vol. 6, p. 202, 1986.

[24] O. Shenfeld, E. Ophir, B. Goldwasser, and A. Katzir, "Silver halide fibre optic radiometric temperature measurement and control of CO_2 laser-irradiated tisues and application to tissue welding," *Lasers Surg. Med.*, vol. 14, pp. 323–328, 1994.

[25] M. C. Oz, R. S. Chuck, J. P. Johnson, S. Parangi, L. S. Bass, R. Nowygrod, and M. R. Treat, "Indocyanine green dye-enhanced welding with a diode laser," *Surgical Forum*, vol. 40, pp. 316–318, 1989.

[26] S. Kuramoto and P. J. Ryan, "First sutureless closure of a colotomy: short-term results of experimental laser anastomosis of the colon," *Dis. Colon. Rectum*, vol. 34, pp. 1079–1084, 1991.

[27] J. Tang, G. Godlewski, S. Rouy, M. Dauzat, J. Juan, F. Chambettaz, and R. Salathe, "Microarterial anastomosis using a noncontact diode laser versus a control study," *Lasers Surg. Med.*, vol. 14, pp. 229–237, 1994.

[28] E. N. LaJoie, "Tissue welding: studies of pulsed diode laser interaction with ICG stained porcine aorta and elastin-based biomaterial," Master's thesis, Oregon Graduate Institute of Science and Technology, 1995.

[29] J. Roider, F. Hillenkamp, T. Flotte, and R. Birngruber, "Microphotocoagulation: selective effects of repetitive short laser pulses," in *Proc. Natl. Acad. Sci. USA*, vol. 90, pp. 8643–8647, 1993.

[30] R. A. Gelman, J. Blackwell, N. A. Kefalides, and E. Tomichek, "Thermal stability of basement membrane collagen," *Biochim. Biophys. Acta.*, vol. 427, pp. 492–496, 1976.

[31] S. Solhpour, E. Weldon, T. E. Foster, and R. R. Anderson, "Mechanism for thermal tissue "welding" (part 1)," *Lasers Surg. Med.*, vol. S6, p. 56, 1994.

[32] F. C. Henriques Jr. and A. R. Moritz, "Studies of thermal injury: the conduction of heat to and through the skin and the temperatures attained therein. A theoretical and an experimental investigation," *Am. J. Path.*, vol. 23, pp. 531–549, 1947.

Biographical Note

Sean D. Pearson was born in Las Cruces, New Mexico on May 2, 1972. He attended New Mexico State University and earned a B. S. degree in Electrical Engineering in May 1994. He has an interest in applying electrical engineering fundamentals to biomedicine, which he pursued at the Oregon Medical Laser Center.